Chapter 3
Molecular Spectroscopy for Exoplanets

Jonathan Tennyson

Abstract One can determine orbital radius, planetary size and planetary mass, and hence average density from techniques used to detect exoplanets. The only real means of expanding on this information is by spectroscopic study of atmospheres. To do this requires a knowledge of the spectroscopy of the molecules, present or likely to be present, in their atmosphere which in turn demands access to the extensive laboratory data that characterises these species. Given that the exoplanets whose spectra can be observed are largely hot compared to our planet, this puts particular demands on spectroscopic data needed both to interpret any observations and to perform radiative transport models of planets of interest. This chapter outlines the basic spectroscopy of atoms and molecules with a particular emphasis on the molecules that likely to form in exoplanetary atmospheres. The importance of treating the temperature dependence of the spectrum and the huge growth in the number of lines which play a role at higher temperatures, such as those deduced for hot Jupiter exoplanets, is emphasized. Sources of data for use in studies of exoplanets are discussed in detail and illustrative examples given.

3.1 General Introduction

The last two decades have taught us that exoplanets are common; indeed it seems that nearly every star supports a planetary system. Logically the next step is to understand more about these newly-discovered bodies. One can determine orbital radius, planetary size and planetary mass, and hence average density from techniques used to make the original detections. The only real means of expanding on this information is by spectroscopic probes of the atmosphere. To do this requires a knowledge of the species, largely molecules, present or likely to be present in the atmosphere. It also requires access to the laboratory data that characterises these species. Given that the exoplanets whose spectra can be observed are largely hot

J. Tennyson (✉)
Department of Physics and Astronomy, University College London,
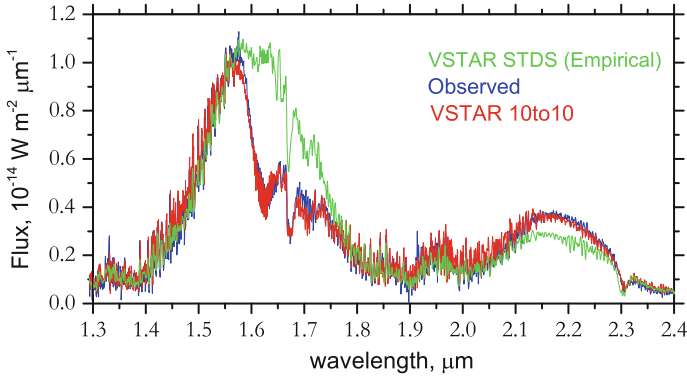London WC1E 6BT, UK
e-mail: j.tennyson@ucl.ac.uk

Fig. 3.1 Spectra of the T 4.5 dwarf 2M 0559-14. The observed spectrum (blue line) was taken with the SpeX instrument on the 3-m NASA Infrared Telescope Facility (IRTF). Models were calculated with VSTAR for $T = 1500$ K using **a** the empirical STDS line list of Wenger and Champion (1998) and **b** the computed 10to10 line list of Yurchenko and Tennyson (2014). The figure is adapted from the work of Yurchenko et al. (2014)

compared to our planet, this puts particular demands on spectroscopic data needed both to interpret any observations and to perform radiative transport models of planets of interest.

Figure 3.1 gives an illustrative example of the importance of using comprehensive sets of spectroscopic data. The example is actually for a methane-rich T-dwarf which provides a better text case since the current status of exoplanet spectroscopy is not good enough to provide a stringent test. The empirical data (STDS) contains a few 100,000 lines while a computed line list contains almost 10^{10} lines. It was found that good results could only be obtained with the inclusion of about 3 billion lines. The need for comprehensive datasets is clear.

This chapter concentrates heavily, but not exclusively, on the spectroscopy of atoms and molecules likely to be found in the atmospheres of exoplanets. A more general introduction to astronomical spectroscopy can be found in my book (Tennyson 2011) of that title. Molecular spectra are governed by the rules of quantum mechanics; my book starts from a basic knowledge of the quantum mechanics of the hydrogen atom to build the rules that govern astronomical spectra and uses observed spectra to illustrate the results. Some knowledge of basic quantum mechanics will be assumed in this chapter. I will survey the underlying nature of molecular spectra giving an idea of the information required to understand them. This survey does little more than give a flavour of the issues involved; for the reader wishing get a deeper or more specialised understanding there are a number of comprehensive text books available of which the book "Spectra of Atoms and Molecules" by Bernath (2015) is an excellent example.

3.1.1 The Basics

Spectroscopy of atoms and molecules probes the energy level structure of these species by absorption or emission of quanta of light, known as photons. These photons possess precisely the right energy to bridge the gap between two energy levels; this is depicted schematically in Fig. 3.2. Because the energy level structure of each atom, ion or molecule is different, the wavelengths of the light absorbed or emitted are unique to that species allowing its identification even over vast distances.

Absorption is the commonest technique used in laboratory high resolution spectroscopy experiments; it requires an appropriate source of light at the wavelengths of interest. This can be hard to arrange in astrophysics but for exoplanets the host star provides a natural light source allowing, for example, absorption spectra to be recorded when a transiting planet moves in front of its host star. Conversely, emission spectra generate their own light by the emitting energy levels becoming overpopulated by thermal or some other means of excitation. The so-called secondary transit probes emissions from a planet's atmosphere.

There is a vast wealth of laboratory spectroscopic data compiled over decades from detailed, high-quality laboratory experiments and, increasingly, from theoretical calculations. Sources of these data are discussed at the end of this chapter. However, exoplanet spectroscopy has raised new challenges for the provision of laboratory data. This is not so much because of the unusual nature of the species: most of the molecules detected, or searched for can be considered to be the usual suspects whose spectra are well-studied on Earth. The issue is to with the environment: first
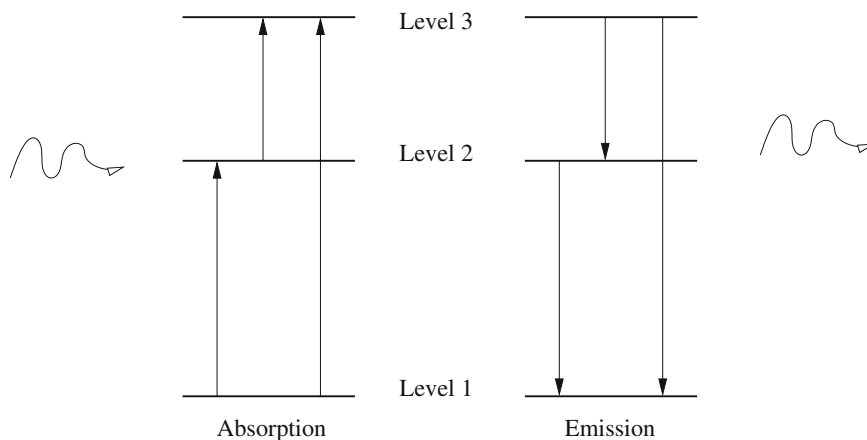

Fig. 3.2 Schematic three-level system showing absorption of an incoming photon (left) or emission of an outgoing photon (right) between the levels. The diagram assumes that transitions between all three levels are allowed, which is often not the case. Note that emission and absorption occur at the same photon wavelength/frequency and that the energy of a photon linking levels 1 and 3 is precisely the sum of the energies of the two photons that link levels 1 and 2, and levels 2 and 3

the exoplanets for which there is any immediate hope of obtaining good spectra are all hot which, as discussed below, can hugely increase the amount of laboratory data needed to analyse or interpret spectra; secondly, at least for gas giant planets, the atmospheres are assumed to be largely composed of molecular hydrogen and atomic helium meaning that collisions effects (pressure broadening) on the spectra of molecules contained therein differs significantly from effects observed in our own atmosphere.

3.1.2 Spectroscopic Regions and Units

Wavelength (λ) and frequency (ν) are related by the speed of light (c) by $\lambda = \frac{c}{\nu}$. Astronomers generally use wavelengths, which have units of length (μm, Å, nm, etc.), in the infrared and visible range as telescopes naturally work in wavelengths. However at the extremes of the spectrum they generally use frequency or energy units, which are closely related. In short wavelength regions, extreme ultraviolet (EUV), X-ray and γ-ray, energy units (usually electron Volts or eV) are generally employed. At long wavelengths such as the radio region which is used to probe the interstellar medium, spectra are usually recorded using frequencies (Hz) although in practice they are often presented as the Doppler shift (in km s^{-1}) from a known laboratory feature. Although this makes sense from the point of view of interpreting motions of clouds etc., it is somewhat bizarre from a spectroscopic viewpoint.

The physics of spectra are most easily understood using energies because this gives a simple relationship between the energy levels and the properties of the transitions. Thus laboratory spectra often use Hz at long wavelengths and eV at very short wavelengths. In the intermediate region, which is the one of most importance for exoplanets, the rather awkward wavenumber units of cm^{-1} are uniformly used. When converting it is worth remembering that a transition at a wavelength of 1 μm has a wavenumber of 10 000 cm^{-1} and they are, of course, inversely related. Figure 3.3 gives an overview of various different units and allows a very approximate conversion between them. Finally it should be noted that astronomers often given energies expressed in units of absolute temperature (K). In this context it is worth noting that 1 K $\approx$ 0.69 cm^{-1}. However one should be careful here because a temperature represents a distribution of energies whereas energy levels and transitions occur at precise values.

Figure 3.3 also shows the various spectroscopic regions of the electromagnetic spectrum. As discussed below the physics of various molecular transitions determines the region in which they can be observed. Conversely the observing strategy is more determined by the spectroscopic behaviour of the Earth's own atmosphere and, of course, there can be issues trying to observe the atmosphere of one planet from inside the atmosphere of another one.
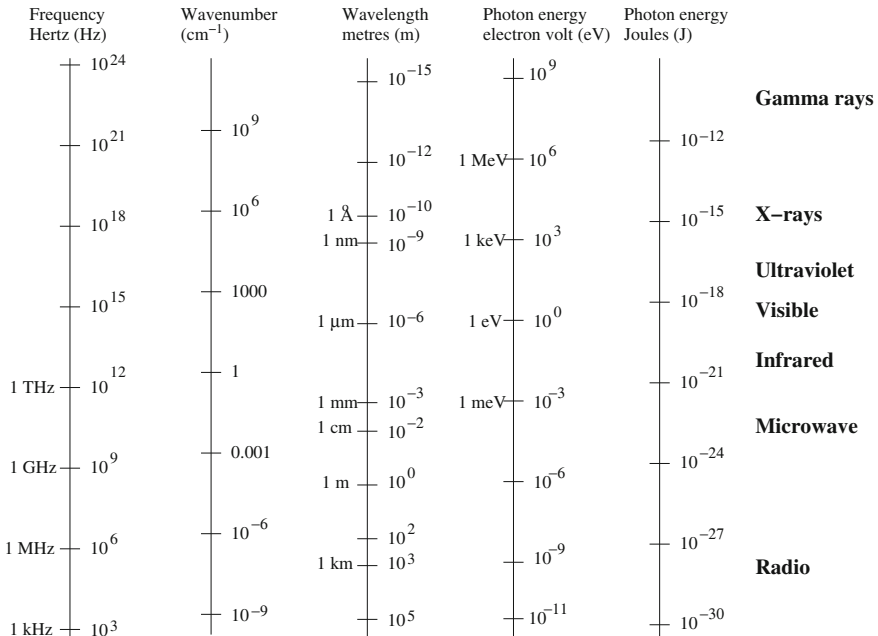
Fig. 3.3 The electromagnetic spectrum

3.1.3 What Does One Learn from an Astronomical Line Spectrum?

The analyses of spectra have provided a wealth of information on the Universe about us. Careful study of spectroscopic data, particularly high-resolution data, can be rich in information about both the chemical and physical characteristics of the object under observation. In particular on can use spectra to determine:

- **Which species produces the line(s)**? This provides information on the chemical composition of the object under observation.
- **Which transition is it**? The comparison of occupancy of ground and excited states gives information about the local physical conditions of the object such as temperature.
- **How strong is the line**? Knowledge of thermal population and transition intensities can be used to reveal the abundance or total column of the species under observation.
- **What is the Doppler shift**? Doppler shifts give information on the motion of the object or region of the object. At high resolution, these data can provide a wealth of information about the local environment of the species.

- **What is the line profile**? Line profiles provide information of the local physical conditions; in principal both the (translational) temperature and the local pressure can be determined from the Doppler and pressure broadening, respectively. Line profiles also provide information on the optical depth.
- **What is the splitting pattern**? Local magnetic fields can be observed via the splitting of spectral lines by the field.

While temperature is one of the most important parameters retrieved from spectral observations, it must be borne in mind that most of the Universe is not in local thermodynamic equilibrium (LTE). Even if observations are well-modeled by a single temperature, this temperature may just represent the effective temperature of a single type of motion such as translation or rotation. Molecules are complicated systems and it is possible to use spectroscopy to determine more than one temperature, see Dello Russo et al. (2005) for example. These different temperatures in turn provide important information about thermalisation timescales.

3.2   Atomic Spectra

Hot objects such as stars with solar temperature ($\approx$5600 K) and above are primarily composed of atomic species at various stages of ionisation. The spectra of these objects are important in their own right as well providing the back drop for exoplanet observations.

In general atomic spectra involve the movement of electrons; one astronomically important exception being the H atom 21 cm line, discussed below, which involves a nuclear spin flip. These electronic transitions are generally strongest at ultraviolet and visible wavelengths. The transitions are observed as discrete lines or groups of lines unlike the bands observed in hot molecules. Nearly all stellar spectra contain prominent atomic features.

All spectroscopic transitions obey selection rules which govern the energy levels which can be reached starting from a given level. As atoms are high symmetry objects they are characterised by a series of quantum numbers which define their states. A discussion of the physics behind these quantum numbers and the rather arcane notation used to represent them can be found in standard textbooks such as Woodgate (1983) and Tennyson (2011).

Table 3.1 summarises the selection rules which give atomic spectra. Electric dipole transitions are generally very much stronger than electric quadrupole or magnetic dipole transitions and, as result, only these transitions are important in the spectra of stars and exoplanets. All dipole allowed transitions must obey the first three selection rules listed but the strongest features, which are the ones usually observed generally obey all the rules listed.

Dipoles usually given in the cgs unit Debye (D). At atomic level, the separation of a unit charge by 1 Bohr (a typical atomic or molecular scale) gives a dipole of 2.54 D.

Table 3.1 Selection rules for atomic spectra. Rules 1, 2 and 3 must always be obeyed. For electric dipole transitions, intercombination lines violate rule 4 and forbidden lines violate rule 5 and/or 6. Electric quadrupole and magnetic dipole transitions are also described as forbidden

	Electric dipole	Electric quadrupole	Magnetic dipole
1.	$\Delta J = 0, \pm 1$	$\Delta J = 0, \pm 1, \pm 2$	$\Delta J = 0, \pm 1$
	Not $J = 0 - 0$	Not $J = 0 - 0, \frac{1}{2} - \frac{1}{2}, 0 - 1$	Not $J = 0 - 0$
2.	$\Delta M_J = 0, \pm 1$	$\Delta M_J = 0, \pm 1, \pm 2$	$\Delta M_J = 0, \pm 1$
3.	Parity changes	Parity unchanged	Parity unchanged
4.	$\Delta S = 0$	$\Delta S = 0$	$\Delta S = 0$
5.	One electron jumps	One or no electron jumps	No electron jumps
	Δn any	Δn any	$\Delta n = 0$
	$\Delta l = \pm 1$	$\Delta l = 0, \pm 2$	$\Delta l = 0$
6.	$\Delta L = 0, \pm 1$	$\Delta L = 0, \pm 1, \pm 2$	$\Delta L = 0$
	Not $L = 0 - 0$	Not $L = 0 - 0, 0 - 1$	

3.2.1 Atomic Hydrogen

As the dominant species in the Universe, the spectrum of atomic hydrogen is of particular importance. H atom spectra obey the selection rules listed in Table 3.1 but, because the H atom only has a single electron this can be significantly simplified. For example, all H-atom states are spin doublets meaning $S = 2$ so the spin selection rule, $\Delta S = 0$ is always satisfied for all transitions.

H atom spectra are divided up into well-known series classified according to the lower energy level involved. These series, which played a crucial role in the early development of quantum mechanics, are listed in Table 3.2. H atom spectra were observed in exoplanets by Vidal-Madjar et al. (2003) via the so-called Lyman α transition which is the transition from the $n = 1$ ground state to the $n = 2$ first excited state. Observation of these lines need to be made in the ultraviolet. Easier to observe from the ground are Balmer series lines; however these transitions start from the excited $n = 2$ state of the H atom which means that the hydrogen must be excited by some mechanism. So far, as discussed by Cauley et al. (2017), detection of Balmer lines has been patchy in exoplanet atmospheres.

Even though every H atom has an electron spin angular momentum of a half, this angular momentum still plays an important role in H-atom spectra. The is because the spin angular moment, $s = \frac{1}{2}$ can couple with the orbital angular momentum, ℓ. For states with $\ell > 0$ (non s states), the resulting total angular momentum, j, can take two, half-integer values given by $\ell + \frac{1}{2}$ and $\ell - \frac{1}{2}$. The splitting of the spectral lines that results from the splitting of the energy levels is known as fine structure. The fine structure effect in atomic hydrogen is summarised in Table 3.3.

There is one more potential source of angular moment in an atom and this is the nucleus. If the nucleus has a non-zero spin then this can also couple with the total electronic angular momentum, j to give the final angular momentum, f.

Table 3.2 Spectral series of the H atom. Each series comprises the transitions $n_2 - n_1$, where $n_1 < n_2 < \infty$

n_1	Name	Symbol	Spectral region	Range/cm^{-1}		
				$n_2 = n_1 + 1$		$n_2 = \infty$
1	Lyman	Ly	Ultraviolet	82257	–	109677
2	Balmer	H	Visible	15237	–	27427
3	Paschen	P	Infrared	5532	–	12186
4	Brackett	Br	Infrared	2468	–	6855
5	Pfund	Pf	Infrared	1340	–	4387
6	Humphreys	Hu	Infrared	808	–	3047

Table 3.3 Fine structure effects in the hydrogen atom: splitting of the nl orbitals due to fine structure effect for $l = 0, 1, 2, 3$. The resulting levels are labelled using H atom notation, and the more general spectroscopic notation of terms and levels (see Sect. 3.4.8)

Configuration	l	s	j	H atom	Term	Level
ns	0	$\frac{1}{2}$	$\frac{1}{2}$	ns$_{\frac{1}{2}}$	$n\,^2$S	$n\,^2$S$_{\frac{1}{2}}$
np	1	$\frac{1}{2}$	$\frac{1}{2}, \frac{3}{2}$	np$_{\frac{1}{2}}$, np$_{\frac{3}{2}}$	$n\,^2$P$^{\mathrm{o}}$	$n\,^2$P$^{\mathrm{o}}_{\frac{1}{2}}$, $n\,^2$P$^{\mathrm{o}}_{\frac{3}{2}}$
nd	2	$\frac{1}{2}$	$\frac{3}{2}, \frac{5}{2}$	nd$_{\frac{3}{2}}$, nd$_{\frac{5}{2}}$	$n\,^2$D	$n\,^2$D$_{\frac{3}{2}}$, $n\,^2$D$_{\frac{5}{2}}$
nf	3	$\frac{1}{2}$	$\frac{5}{2}, \frac{7}{2}$	nf$_{\frac{5}{2}}$, nf$_{\frac{7}{2}}$	$n\,^2$F$^{\mathrm{o}}$	$n\,^2$F$^{\mathrm{o}}_{\frac{5}{2}}$, $n\,^2$F$^{\mathrm{o}}_{\frac{7}{2}}$

This splitting, which is usually very small, is called hyperfine structure. For the H atom the nuclear spin, i, is a half. The H atom ground state, the 1 s state, has $j = \frac{1}{2}$ and coupling with i gives allowed f of 0 and 1. This splitting is very small but it is still possible to observe the very weak $f = 0 - 1$ line which lies in the radio region with a wavelength of $\lambda = 21$ cm. The 21 cm line is arguable the most important single line in astronomy. It can be used to map H distributions and velocities throughout the Universe. Its weakness means that the line is rarely saturated which allows H atom columns to be recovered with confidence.

3.2.2 Helium Spectra

Helium is of course the second most abundant species in the Universe. However observing it is much more difficult than for H. In a large part this is due to its atomic structure. He is a closed shell species with two electrons in the lowest orbital ($1s^2$ in standard atomic physics notation). The leading, 'resonance', line is the 1s2p – $1s^2$ transition that occurs at about 20 eV (more precisely at $\lambda = 584$ Å). This lies well into the ultraviolet requiring both a high energy light source to drive the transition and making its observation from the ground impossible. Furthermore, the line is

obscured by interstellar H atoms which absorb at 584 Å. It will therefore be very hard to perform a direct, spectroscopic detection of He in the atmosphere of an exoplanet.

3.2.3 Complex Atoms

The spectra of many-electron atoms are more complicated than of hydrogen and the full atomic selection rules, as given in Table 3.1, come into play. For stellar and exoplanet spectra of these species, magnetic dipole and electric quadrupole transitions are so weak that they can safely be ignored. Electric dipole transitions can be divided into three classes. Strong, fully-allowed transitions obey all the rules specified. However, strictly dipole transitions only have to obey the first three selection rules concerning changes in ΔJ, ΔM_J and parity. The final rule is often known as the Laporte rule after its discoverer.

Transitions which obey all six selection rules are known as "allowed". Lines which satisfy all the rules except spin selection rule 4 ($\Delta S = 0$) are called intercombination lines and lines which violate selection rule 5 and/or 6 are known as "forbidden" lines. This last nomenclature is somewhat confusing as forbidden lines do occur and indeed give strong emissions in interstellar environments. However, they are generally too weak to concern us here. Similarly, intercombination lines, while generally stronger than forbidden lines are also too weak to be significant in planetary or stellar atmospheres.

Besides atomic hydrogen discussed above the main atoms detected in exoplanet atmospheres are the alkali metal atoms Na and K. For example, Pont et al. (2013) give a robust detection on exoplanet on HD189733b of Na and K lines at 0.589 μm and 0.769 μm, respectively. Alkali metals have a single "valence" electron outside a closed shell core and it is the movements this electron, alone, which gives alkali atoms their characteristic spectra.

Table 3.4 summarises the various spectral lines grouped into series. The names of these series are the origin of a nomenclature which denotes atomic orbital with 0, 1, 2 and 3 units of angular momentum s, p, d and f, respectively. The spectrum of K has a similar structure just shifted to sightly longer wavelengths. Conversely the atomic ion Mg^+ (or Mg II in standard atomic physics notation) is isoelectronic (has the same number of electrons) as Na so also displays a spectrum with very similar structure but shifted to significantly shorter wavelengths. Transitions from these species are also prominent in stellar atmospheres.

An important feature shown in Table 3.4 is the splitting of lines due to spin-orbit effects. These doublets and triplets are usually resolved in astronomical objects and can be used to determine effects such as optical thickness as the relative strengths of different transitions within a multiplet is determined by the underlying atomic physics when the lines are observed optically thin.

Table 3.4 Spectral series of sodium

Series name	Transitions	n values	Multiplicity
Sharp	$n\,^2S_{\frac{1}{2}} \to 3\,^2P^o_{\frac{3}{2},\frac{1}{2}}$	$n = 4, 5, 6, \ldots$	Doublets
Principal	$n\,^2P^o_{\frac{3}{2},\frac{1}{2}} \to 3\,^2S_{\frac{1}{2}}$	$n = 3, 4, 5, \ldots$	Doublets
Diffuse	$n\,^2D_{\frac{5}{2},\frac{3}{2}} \to 3\,^2P^o_{\frac{3}{2},\frac{1}{2}}$	$n = 3, 4, 5, \ldots$	Triplets
Fundamental	$n\,^2F^o_{\frac{7}{2},\frac{5}{2}} \to 3\,^2D_{\frac{5}{2},\frac{3}{2}}$	$n = 4, 5, 6, \ldots$	Triplets

3.2.4 Atoms (and Molecules) in Magnetic Fields

The presence of a magnetic field can cause splitting in observed spectra of atoms and molecules. These spectra, in which splittings are not always fully resolved, therefore provide the means to determine the strength of the local magnetic field. While all atomic and molecular spectra are affected by a magnetic field to some extent, the strongest effects are observed in the spectra of open shell atoms such as the spectra of Na and K discussed above.

For a so-called weak magnetic field, B, the splitting of the spectral lines is known as the Zeeman effect and takes the fairly simple form:

$$\Delta E = M_J \mu_B g_J B, \tag{3.1}$$

where μ_B is the Bohr Magneton, the basic quantum of magnetic effects, which is defined by

$$\mu_B = \frac{e\hbar}{2m_e} \tag{3.2}$$

where e and m_e are the charge and mass of the electron. and $\hbar$ is Planck's constant divided by 2π; this means $\mu_B = \frac{1}{2}$ in atomic units. J is the total angular momentum of the system and M_J is projection of J along the direction of the magnetic field; M_J takes $(2J + 1)$ values for $-J \leq M_J \leq J$ in steps of 1. Finally g_J is the so-called Landé g-factor which captures the strength of the interaction of the levels of the particular species with the magnetic field. For closed shell molecules such as H_2O, CH_4 etc., g_J is very small; it is more significant for open shell diatomics such as TiO, VO, C_2. As mentioned above, the largest g-factors are generally for open shell atoms. Introducing a magnetic field results in splitting of the levels characterised by M_J. Transitions between these levels are governed by the rule $\Delta M_J = 0, \pm 1$, see Table 3.1. Atomic spectra have widely been used to characterise the magnetic fields present in stars. People interested in a detailed exposition of this topic should look at the work of Berdyugina and Solanki (2002). Similar studies should become possible for exoplanets as spectral resolution improves.

Strong magnetic fields have a more radical effect on the level structure of atoms and molecules. This is governed by the so-called Paschen-Back effect. A discussion of the role and study of this effect in astrophysics is given by Berdyugina et al. (2005).

3.3 Molecular Motions

The spectra of molecules are more complicated and richer than those of atoms. Understanding them involves probing deeper into underlying physics as the changes induced by absorbing or emitting a photon now involve movement of the nuclei as well as, in some cases, changes in the electronic structure. Before considering the different types of molecular spectra, it is necessary to consider the different degrees of freedom available to the nuclei in a given molecule.

Consider a molecule containing N atoms. In simple Cartesian space each atom has 3 degrees of freedom so the molecule as a whole has $3N$ degrees of freedom. The bonding in the molecule puts constraints on the motions of the individual atoms and it is better to consider these degrees of freedom as a collective property of the whole molecule rather than of individual atoms. Doing this gives the following.

The translation of the whole molecule through space can be undertaken in 3 dimensions so there are 3 translational degrees of freedom. These yield essentially a continuous set of translational levels which are not of interest spectroscopically. Fortunately it is reasonably straightforward to re-write the molecular Hamiltonian to formally separate this translation motion and from here on I will assume that this has been done.

In addition to translation, the whole molecule can rotate freely in space. If the molecule is linear it can do this only the two directions perpendicular to linear structure; otherwise it will rotate in all 3 dimensions. Unlike the translation motion, the rotational motion is quantized and can be probed spectroscopically. This is discussed below.

Having identified 6 (5 for a linear molecule) degrees of freedom associated with the collective motion of the entire system, there remain $3N - 6$ ($3N - 5$ for a linear molecule) degrees of freedom which are associated with internal motions of the system. These motions are called vibrations and involve the atoms vibrating against each other. These motions are generally represented using $3N - 6$ ($3N - 5$) internal coordinates. For diatomic molecules this reduces simply to a single internal coordinate which is the one used to represent the well-known potential energy curves describing the interaction between the two atoms in the molecules. Examples of these are given below.

As for atoms, spectra can also arise due to changes (jumps) in the electronic structure of a molecule. In general these electronic changes are similar to those found in atoms but with complications due to the lower symmetry and the fact that the nuclear motion also participates in electronic transitions.

Fig. 3.4 Schematic diagram illustrating the Cartesian principal axes of rotation for an arbitrary solid body. By convention the axis with the smallest moment of inertia is labelled A and the one with the largest moment inertia is labelled. C
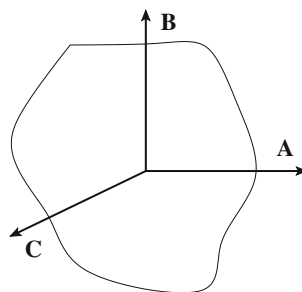
So for molecules there are three distinct quantized motions that can give rise to spectra: rotational motion, vibrational motion and electronic motion. Each of these possible spectra, which are discussed each in turn below, lie in a different, characteristic spectral region.

With the exception of the spectra associated with the abundant molecular hydrogen, H_2, it is only necessary to consider molecular transitions governed by electric dipole selection rules. However, molecules have an extra source of dipole moment in form of the configuration of the various nuclei in the molecule which can give rise to both permanent and instantaneous dipoles which then facilitate transitions.

3.4 Rotational Spectra

The simplest spectrum to arise from molecules is the rotational spectrum. Studies of these spectra have provided a vast amount of information of the interstellar medium and star-forming regions.

The simplest way to understand rotational spectra is to start by considering the molecule as a rigid rotor. A rigid system rotates about its so-called principal axes, see Fig. 3.4. These axes are obtained, at least in principle, by diagonalising its moment of inertia tensor. This may sound complicated but for many small molecules, such as water, the orientation of the principle axes is intuitive as it is completely determined by symmetry. Principal axes are used to represent both the classical and quantum mechanical rotational motion of solid bodies.

If the body is rigid then quantum mechanically the rotational energies levels of the system can be characterized by the rotational constant which is directly related to the component of the moment of inertia, I_X, associated with the given principal axis:

$$B = \frac{\hbar^2}{I_B}. \tag{3.3}$$

Clearly there are three possible rotational constants, denoted A, B and C. By convention, the constants are assumed to have the order $A \leq B \leq C$. As shown in the

following subsections, these constants are used to classify the different types of possible molecular rotors.

Electric dipole-allowed rotational spectra generally require the molecule to possess a permanent dipole moment, usually denoted μ. This moment arises from the asymmetry of the charge distribution in the molecule. The intensity of the associated rotational transitions is proportional to $|\mu|^2$, so the magnitude of this dipole plays an important role in the observability of any transitions.

Pure rotational spectra obey the rather simple, general angular momentum selection rule $\Delta J = -1, (0), +1$, where $\Delta J = 0$ transitions can only occur non-trivially for systems with multiple energy levels for a given J. In practice, such transitions are important for asymmetric top molecules, see below.

The energy taken to excite a rotational level is relatively small meaning that transitions occur at long wavelengths. Many molecules show characteristic rotational spectra at radio frequencies while lighter molecules absorb and emit in the far infrared.

Rotational motions can be represented relatively easily: a basis of the $(2J + 1)$ rotational functions given by the Wigner rotation matrices are sufficient to characterise all levels for a given J. In practice parity can be used to symmetrise this basis into two sets of $(J + 1)$ and J functions. More information is given in specialist texts such as Bernath (2015).

In order to appreciate the rotational spectrum of different molecules it is necessary to first classify these species to different types of rotor. This is done on the basis of their moments of inertia, or, more usually, the rotational constants derived from them. This analysis shows that molecules can be classified into four classes of rotor. These are considered in turn below.

3.4.1 Linear Molecules

Linear molecules can only rotate about two axes and are therefore characterized by the rotational constants $A = 0$ and $B = C$. All diatomic molecules, including of course the abundant H_2 and CO molecules, are linear. A number of important polyatomic species such CO_2, HCN and HCCH are also linear.

The rotational energy levels of a rigid linear molecule are given by the formula

$$E_J = BJ(J + 1). \tag{3.4}$$

Using this formula with the $\Delta J = 1$ selection rule leads to the result that the rotational transitions are uniformly spaced in frequency/wavenumber/energy at intervals of $2B$. In practice molecules are non-rigid so this spacing actually decreases (slightly) with increasing J. However the uniform nature of the spectrum is easily recognised, see Fig. 3.5.
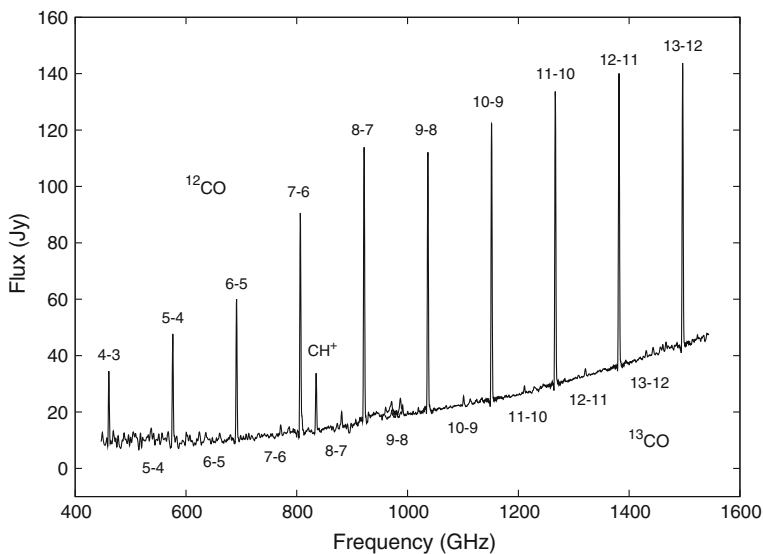
Fig. 3.5 Rotational spectrum of carbon monoxide (CO) recorded in emission from planetary nebula NGC 7027 using the using the SPIRE Fourier Transform Spectrometer on the Herschel Space Observatory. Note the even spacing between rotational transitions. (Adapted from R Wesson et al., *Astron. Astrophys.*, **518**, L144, 2010)

As already discussed, strong transitions require a dipole moment and for rotational transitions this is provided by the permanent dipole moment of the molecule. However, not all linear molecules have a permanent dipole. So-called homonuclear diatomic molecules such as H_2 and N_2 have zero dipole, as do symmetric linear polyatomic species such as CO_2 and HCCH. However, many important linear molecules do have a permanent dipole including all heteronuclear diatomic molecules such as CO and NaCl. Asymmetric linear polyatomic molecules such as HCN also have dipoles. As linear molecules concentrate all the intensity for transitions between neighbouring J levels into a single spectral line, their spectra tend to be strong. This is even true for the important CO molecule which actually possesses a rather small dipole moment.

The non-rigidity of the molecule leads to effects due to centrifugal distortion: the bond in the molecule stretches slightly as the molecule rotates. This leads to a small lowering in the rotational energy levels and a corresponding closing up of the transition frequencies. This effect can be represented as a power series expansion obtained using perturbation theory starting from the idea that rotations are rigid. Adding the leading correction to Eq. 3.4 gives:

$$E_J = BJ(J+1) - DJ^2(J+1)^2 + \cdots \tag{3.5}$$

which shows that centrifugal effects become much more pronounced at high J values.

Of course molecules also vibrate which means that rotational constants such as B and D also depend on the vibrational state of the molecule. This means that more generally expression (3.5) is written

$$E_J^v = B_v J(J+1) - D_v J^2 (J+1)^2 + \cdots \tag{3.6}$$

where E_J^v represents the rotational energy of vibrational state v. The rotational constants B_v and D_v then also depend on the vibrational state with B_0 and D_0 characterizing the rotational energies of the ground (lowest) vibrational state. Rotational line positions both in the lab and astronomically can often be measured to high accuracy which involves extending the treatment given above. This is discussed in standard textbooks on molecular spectroscopy such as Bernath (2015).

Huber and Herzberg (1979) gave a comprehensive and very useful compilation of constants of diatomic molecules which is now available, unupdated, via the NIST chemistry web book (http://webbook.nist.gov/chemistry). This is a valuable, but dated resource.

3.4.2 Spherical Tops

Spherical top molecules are characterized by having all three rotational constant the same, $A = B = C$. This is the same property as any sphere and actually means that the orientation of the principle axes is arbitrary. The energy levels of spherical tops obey formulae similar to those for linear molecules discussed in Sect. 3.4.1 above. Astronomically important examples of spherical top molecules include methane (CH_4), silane (SiH_4) and buckminster fullerene (C_{60}).

The lack of any unique orientation for spherical top molecules means that they cannot possess a permanent dipole moment. This means that spherical tops should not undergo pure rotational transitions. In practice, as the molecule rotates it undergoes centrifugal distortion about the axis of rotation. This can induce a small, temporary dipole moment and leads to a weak rotational spectrum. Molecules containing hydrogen are easier to distort in this fashion and weak rotation spectra for methane are well-known, see Bray et al. (2017). However, they are likely to be too weak to be of great importance for exoplanetary spectroscopy.

3.4.3 Symmetric Tops

Symmetric top molecules have two moments of inertia which are identical and one which is different. They therefore occur in two distinct forms:

1. Prolate for which $A > B = C$. Prolate species can be thought of as egg-shaped.
2. Oblate for which $A = B > C$. Extreme oblate tops are flat like a disk. The planar symmetric molecule H_3^+ is an example of an oblate symmetric top.

The energy levels of a symmetric top are characterised by two quantum numbers, the usual J and K, which is the projection of J along the symmetry axis of the molecule. This extra quantum number lifts the $(2J + 1)$ degeneracy of the energy levels found for the rigid symmetric top. Since $|K| \leq J$, there are now $J + 1$ distinct levels. The level with $K = 0$ is singly degenerate and all other levels are two-fold degenerate.

The energy levels of a rigid prolate symmetric top can be written

$$E_J = BJ(J + 1) + (A - B)K^2, \tag{3.7}$$

while those for a rigid oblate symmetric top are

$$E_J = BJ(J + 1) + (C - B)K^2. \tag{3.8}$$

Transitions follow the general $\Delta J = 1$ selection with the strong propensity that K does not change, *i.e.* $\Delta K = 0$.

Most symmetric tops, including molecules like ammonia (NH_3) and phosphine (PH_3) have permanent dipole moments and hence rotational spectra. Figures 3.6 and 3.7 show room temperature rotational spectra of NH_3 and PH_3, respectively. The regular structure due to the $\Delta J = 1$ transition rule is clearly seen; the broadening of the features which can be seen at higher frequencies (high J) is due to the K substructure.

Planar symmetric-top molecules, such as H_3^+, do not possess a permanent dipole. However, H_3^+, like methane, is predicted to have a 'forbidden' rotational spectrum, see
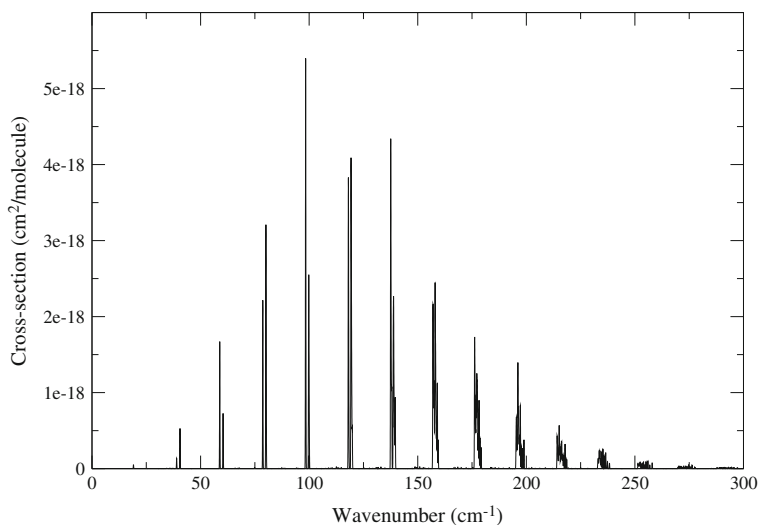

Fig. 3.6 Rotational spectrum of ammonia (NH_3) at 296 K generated using the BYTe line list of Yurchenko et al. (2011)
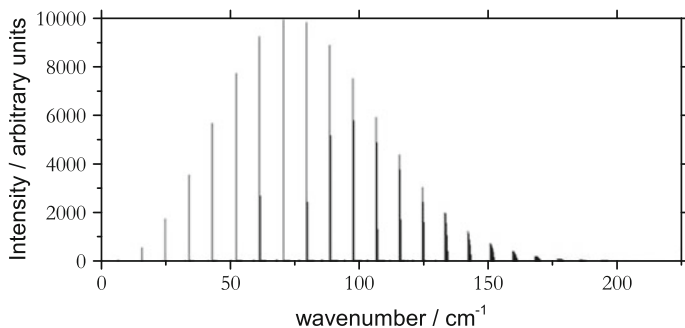
Fig. 3.7 Rotational spectrum of phosphine (PH_3) at 296 K generated using the line list of Sousa-Silva et al. (2013)

Miller and Tennyson (1988). This spectrum has yet to be observed in the laboratory or space but there is so much H_3^+ in environments such as Jupiter's aurora that it should be observable. However, the most prominent transitions lie in the far-infrared making them difficult to observe from Earth.

3.4.4 Asymmetric Tops

Asymmetric top molecules are characterized by having all moments of inertia different and in this case $A > B > C$. There are many asymmetric top species; common astronomical examples include water (H_2O) and formaldehyde (H_2CO). For both of these species it is possible to place the principle axes of rotation uniquely on symmetry grounds. For many molecules, such as ethanol (CH_3CH_2OH) this is not so and these axes plus their associated rotational constants have to be obtained by explicit diagonalisation of the moment of inertia tensor.

Asymmetric tops completely break the $(2J + 1)$-fold degeneracy of each J level found in symmetric tops and therefore require a new notation for the energy levels. In practice there are two notations. The more common one uses the projection of the rotational angular momentum, J, along the A and C axes giving approximate quantum numbers K_A and K_C, respectively. The states are generally denoted $J_{K_A K_C}$ e.g. 1_{10}. An alternative, more compact notation, uses τ which is defined as $\tau = K_A - K_C$. In this notation the $(2J + 1)$ levels run from $\tau = -J$ (lowest) to $\tau = +J$ (highest) and are denoted J_τ.

Even within the rigid rotor approximation the formula for the energy levels of an asymmetric top cannot in general be represented in a simple analytic form and the reader is referred to specialist books, such as Townes and Schawlow (2012), for more information.

The splitting of the energy levels results in asymmetric tops observing the more general selection rule that $\Delta J = 0, \pm 1$ meaning that transitions are allowed between

different $K_A K_C$ within a given J. Although it is possible to find asymmetric tops without a permanent dipole, such as ethyne (CH_2CH_2) and ethane (CH_3CH_3), these are rare. Most asymmetric tops have a permanent dipole moment and complicated rotational spectra with little discernable pattern to them. A classic example is water whose spectrum spreads across large regions of the far infrared in a manner for which little or no systematic structure is readily apparent, see Fig. 3.8.

Rotational spectra of hot water can clearly be seen in a variety of locations. The spectrum of cold water is heavily obscured by water vapour in our own atmosphere and so cannot be observed from the ground. In contrast, however, much of the spectrum of hot water is shifted into the so-called water windows and so the spectra of hot water in astronomical sources can be observed from the ground. Figure 3.9 shows a small portion of a very detailed spectrum of a sunspot recorded from the Kitt Peak National Observatory.

3.4.5 Molecular Hydrogen

Molecular hydrogen, H_2, is a linear molecule with no permanent dipole moment. For rotational spectroscopy that should be the end of the matter but because the abundance of hydrogen in the Universe is so large it is necessary to consider all possibilities. Of course, gas giants are largely composed of hydrogen so its spectrum is very important for exoplanets.

Changing one H atom for a deuterium (D) creates an asymmetry. HD itself has a very small dipole moment of about 5×10^{-4} D, see Pachucki and Komasa (2008).
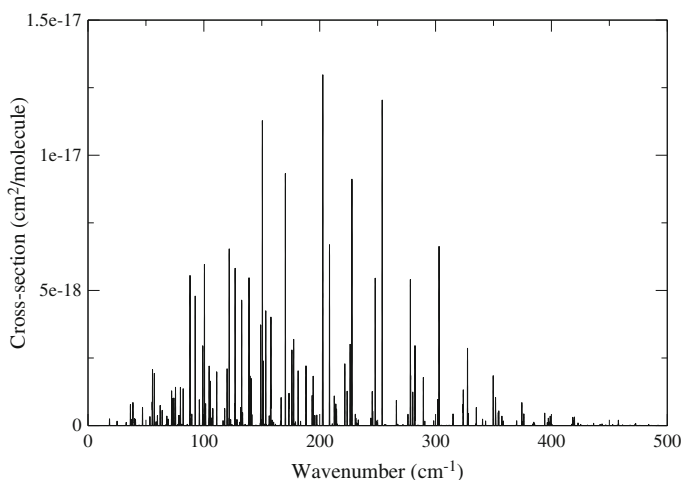

Fig. 3.8 Rotational spectrum of water at 296 K generated using the BT2 line list of Barber et al. (2006)
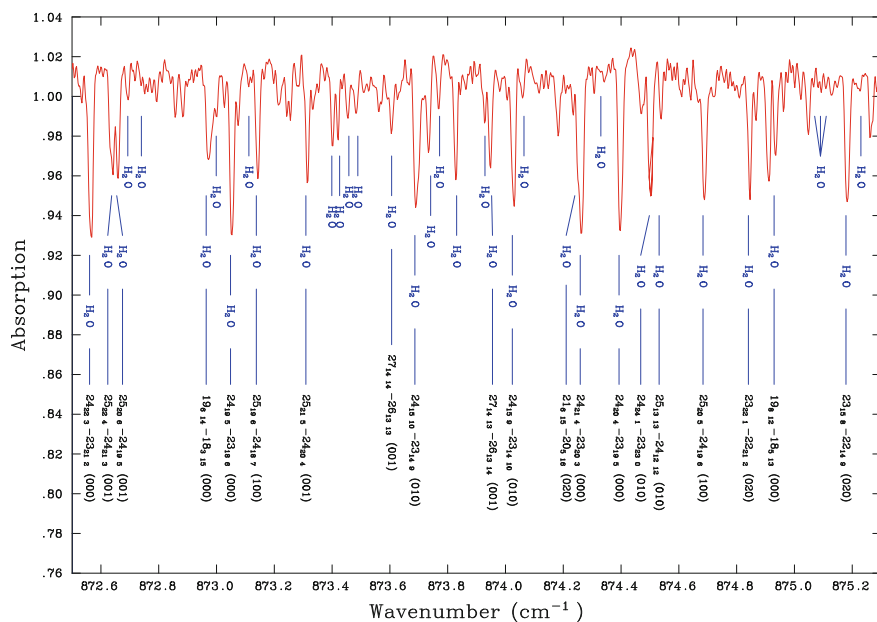
Fig. 3.9 Absorbtion spectrum of water recorded in sunspots by Wallace et al. (1996) with line assignments due to Polyansky et al. (1997)

The ionised form of HD, HD^+ has a much larger permanent dipole moment due to the separation between the centre-of-mass and centre-of-charge. A simple back-of-the-envelope calculation suggests that this should be about 0.85 D. As the transition intensity scales as the square of the dipole moment, HD^+ should be hugely easier to see than HD. However, so far the dipole-driven rotational spectrum of neither has been observed in space.

Turning to H_2 itself, this can be observed through very weak electric quadrupole transitions. Such transitions are about 10^8 times weaker than standard electric dipole transitions but clearly visible in space given the large columns of H_2. In fact it is much easier to see H_2 rotational transitions in space than in the lab!

Quadrupole transitions have the selection rule $\Delta J = 0, \pm 2$. Given that the rotational constant for H_2, B, equals 60.853 cm^{-1}, these transitions lie in the far infrared. In particular:

$J = 2 - 0$ lies at 28.22 μm;
$J = 3 - 1$ lies at 17.04 μm;
$J = 10 - 8$ lies at 5.05 μm.

These lines and many more have been observed in a variety of locations but not yet in exoplanets.

3.4.6 Isotopologues

Isotopologues are isotopically substituted molecules such as ^{13}CO for example. Rotational spectroscopy is the best way of detecting isotopologues and hence determining isotopic abundances. This is because there is a direct relationship between the rotational constant, B, and the mass of the atoms.

The rotational constant can be defined in terms of the moment of inertia, I, as:

$$B = \frac{\hbar^2}{2I} \tag{3.9}$$

The moment of inertia itself depends on the molecular (reduced) mass, μ, via the relationship

$$I = \mu R^2 \tag{3.10}$$

where R is the (effective) bondlength. For diatomic molecule such as CO the reduced mass is

$$\mu = \frac{M_C M_O}{M_C + M_O}. \tag{3.11}$$

This means changing from, for example, ^{12}C^{16}O to ^{13}C^{16}O gives a significant shift in line position:

$J = 1 - 0$: $\lambda(^{12}\text{C}^{16}\text{O}) = 2.60$ mm
$J = 1 - 0$: $\lambda(^{13}\text{C}^{16}\text{O}) = 2.72$ mm

Such shifts are straightforward to observe and, as a result, pure rotational spectra give the most sensitive method of studying astronomical isotope abundances.

3.4.7 Temperature Effects

Molecular spectra show strong temperature effects and can provide a useful thermometer in many astronomical environmemts. Except in the very coolest environments, molecules are usually found occupying a range of rotational energy levels. In thermodynamic equilibrium, the occupancy of a given level, P_i is determined by Boltzmann's distribution:

$$P_i = \sum_i \frac{g_i \exp\left(-\frac{E_i}{kT}\right)}{Q(T)} \tag{3.12}$$

where the sum runs over all levels, i, of energy E_i (with $E_0 = 0$) and degeneracy g_i. T is the temperature and k is Boltzmann's constant. $Q(T)$ is the partition function which is given by

$$Q(T) = \sum_i g_i \exp\left(-\frac{E_i}{kT}\right). \tag{3.13}$$

The partition function both keeps the probability of occupancy normalised and provides information on distribution of energy levels.

Partition functions are important for determining the behaviour of molecules as a function of temperature. At elevated temperatures one needs to be careful when computing them as the sum must run over many, may be all, levels in the system, see Vidler and Tennyson (2000). Gamache et al. (2017) give partition functions up to $T = 3000$ K for molecules occurring in the Earth's atmosphere. Barklem and Collet (2016) present partition functions for 291 diatomic molecules and atoms of astrophysical interest which updates but does not entirely replace earlier compilations by Irwin (1981) and Sauval and Tatum (1984). Finally the ExoMol database, see Tennyson et al. (2016c), contains partition functions that extend to high temperatures for all ExoMol molecules, see Table 3.6.

In the absence of a magnetic field, rotational states have degeneracy factor $g_J = (2J + 1)$ which means that the $J = 0$ state is not generally the most populated one. Instead the highest populated J state, $P_J^{(\max)}$, is given by the formula

$$P_J^{(\max)} = \frac{kT}{2B} - \frac{1}{2} \tag{3.14}$$

3.4.8 Data Sources

As mentioned above Huber and Herzberg (1979)[1] give data on rotational spectra of diatomic molecules. CDMS (The Cologne Database for Molecular Spectroscopy) (www.astro.uni-koeln.de/cdms) of Müller et al. (2005) and the JPL Molecular Spectroscopy database (spec.jpl.nasa.gov) due to Pickett et al. (1998) provide largely complementary information on spectra of a large range of astrophysically-important molecules at long wavelengths. As such the data are mainly concerned with the rotational spectra of these molecules. The virtual atomic and molecular data centre (VAMDC) provides a portal with access to a variety of data sources including CDMS and JPL, see Dubernet et al. (2016).

3.4.9 Other Angular Momentum

There are other sources of angular momentum in molecules. The full coupling can become complicated, see Brown and Carrington (2003). One of these sources of angular momentum is the spin of the nuclei. Because coupling between the rotational motion of the molecule and the nuclear spin is weak, the splitting of spectral lines due to it is small and is known as the hyperfine structure. The large splitting due to coupling to any electronic angular momentum is generally called fine structure.

---

[1]Available at http://webbook.nist.gov/chemistry.

Fig. 3.10 Long-wavelength
transitions between
low-lying states in the OH
molecule. The basic splitting
of the rotational levels are
due to spin-orbit coupling
and represent fine structure.
The expanded region shows
the resolved hyperfine
transitions within the lowest
rotational transition
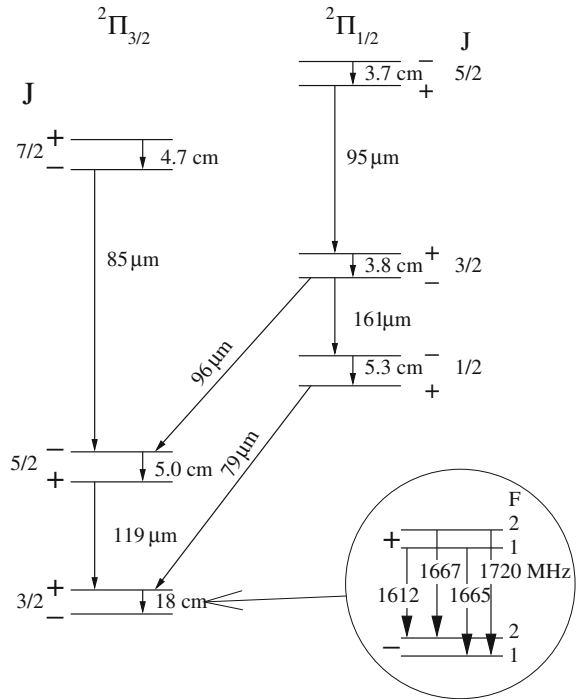
If the nuclear spin angular momentum is denoted I, the final angular momentum, F, can take values $F = |J - I|, |J - I + 1|, \ldots J + I - 1, J + I$. This hyperfine structure is quite often resolved in astronomical spectra; Lellouch et al. (2017) report such observation for HCN in the atmosphere of Pluto, for example. Remarkably, in some case it has been observed to be out of thermodynamic equilibrium.

Figure 3.10 shows the energy level splitting and long wavelength transition in the OH molecule illustrating both fine and hyperfine structures.

3.5 Vibrational Spectra

Vibrational spectra usually lie in the infrared and are important for the atmospheric properties of planets. Indeed, it is through the use of infrared vibration-rotation spectra (all vibrational spectra involve simultaneous changes in rotation) that nearly all detections of molecules in exoplanets have been made so far.

As discussed above, molecules vibrate with $3N - 6$ ($3N - 5$ for a linear molecule) degrees of freedom, which are generally termed vibrational modes. These vibrations represent generally small displacements from the equilibrium structure of the molecule.

The simplest assumption which works well in many cases is to assume that the vibrations are harmonic. The energy levels for the harmonic oscillator follow the rule:

$$E_v = \hbar\omega(v + \frac{1}{2}) \tag{3.15}$$

where v is the vibrational quantum number and ω is the angular frequency. In terms of molecular properties ω is given by

$$\omega = \left(\frac{k}{\mu}\right)^{\frac{1}{2}} \tag{3.16}$$

here k is the force constant as classically given by Hooke's law and μ is the reduced mass, which has already been discussed above for rotation.

Within the harmonic approximation, the vibrational modes are generally known as normal modes of vibration. Although changes of state by a single vibrational quantum usually gives the strongest transitions, other vibrational transitions are allowed and there is a standard terminology for describing these harmonics:

v_1: $(1,0,0,\dots) - (0,0,0,\dots)$, the fundamental band;
nv_1: $(n,0,0,\dots) - (0,0,0,\dots)$, overtone band, $n > 1$;
$nv_1 + mv_2$: $(n,m,0,\dots) - (0,0,0,\dots)$, combination band;
$nv_1 - mv_1$: $(n,0,0,\dots) - (m,0,0,\dots)$, hot band, $n > m > 0$;
$nv_1 - mv_2$: $(n,0,0,\dots) - (0,m,0,\dots)$, difference bands.

These transitions are not subject to any rigorous selection rules on the change in vibrational quantum numbers. Generally changes with $\Delta v = 1$, such as in the fundamental, are much the strongest. But this is not always true: for example the important H_3^+ molecule has a very strong $\Delta v_2 = 2$ bending overtone which happens to lie in the K-band allowing it to be observed from ground-based telescopes; indeed the original spectroscopic detection of H_3^+ in Jupiter by Drossart et al. (1989) was based on a very strong K-band emission spectrum.

Vibrational transitions are usually accompanied by changes in the rotational quantum number. These changes mean that a vibrational transition gives a band with a characteristic structure rather than just a single line. For all bands, transitions which satisfy the selection rule $\Delta J = 1$ are allowed. $\Delta J = J' - J'' = -1$ transitions (where J' is the upper level and J'' the lower one) are called the P branch and often labelled P(J''). $\Delta J = +1$ transitions give the R branch with individual transitions labelled R(J''). In cases where $\Delta J = 0$ transitions are also allowed then the band also shows a Q branch which often manifests itself as a strong feature made up of many overlapping transitions near the band centre.
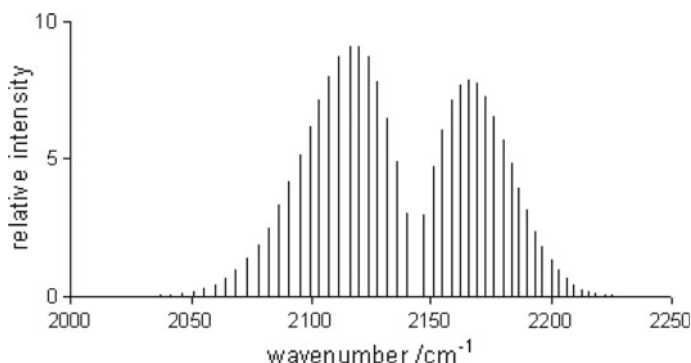
Fig. 3.11 The fundamental band of the CO molecule clearly showing the P-branch at frequencies below the band centre and R-branch at higher frequencies. The actual band centre is given by the missing line

3.5.1 Diatomic Molecules

Diatomic molecules only have one vibrational mode. Their spectra usually have a rather simple structure with a clearly visible P-branch at a lower frequency than the band centre and an R-branch at higher frequencies. Within the these two branches, transitions involving successive J levels are separated by approximately $2B$. In the absence of a Q-branch, the band centre is characterised by a gap of approximately $4B$ between the two branches. Figure 3.11 shows an example for the fundamental band of CO which clearly shows this structure.
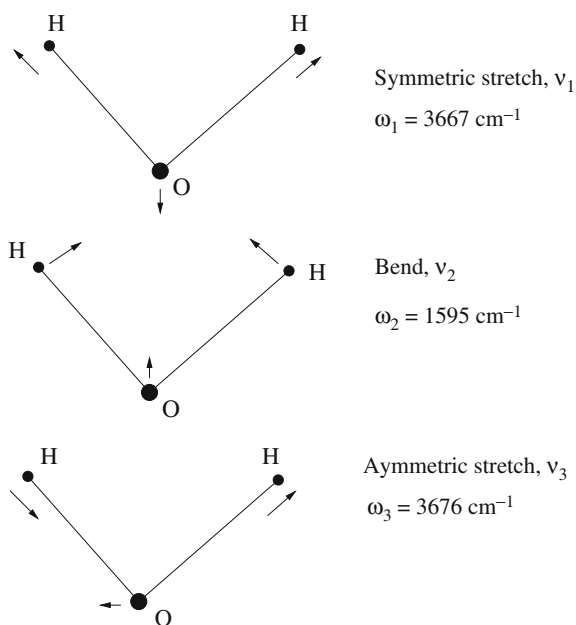
The intensity of vibrational spectra relies on the change in the dipole moment upon vibrational excitation. Diatomics comprising two identical atoms, homonuclear diatomics, have zero dipole moment for internuclear separations so the dipole cannot change with vibrational change as it is always zero. These molecules do not have dipole allowed vibration-rotation spectra. All other diatomic molecules, heteronuclear diatomics, do have allowed spectra which, as discussed, generally lie in the mid-infrared although overtone bands can extend into the far-infrared.

3.5.2 Polyatomic Molecules

For molecules with more than two atoms it is necessary to specify the normal modes of vibration. Figure 3.12 illustrates this with the three normal modes for water.

Figure 3.12 also gives the vibrational frequencies, in the standard wavenumber units of cm^{-1}, for the fundamental modes of the water molecule. I note that $\omega_1 \approx \omega_3$ and $2\omega_2 \approx \omega_1 \approx \omega_3$. This observation has important consequences for the infrared spectrum of water as it means that bands associated with these motions overlap giving rise to what is know as polyad structures in the spectrum.

Fig. 3.12 Schematic representation of the water normal modes of vibration. Also given is the fundamental frequency of each mode

Symmetric stretch, ν_1

$\omega_1 = 3667$ cm^{-1}

Bend, ν_2

$\omega_2 = 1595$ cm^{-1}

Aymmetric stretch, ν_3

$\omega_3 = 3676$ cm^{-1}

For water, the polyad number N of any vibrational state is given by $n_1 + \frac{1}{2}n_2 + n_3$ where n_1, n_2 and n_3 are the numbers of quanta of excitation of the respective vibrational modes. Polyad nomenclature varies from molecule to molecule; for water the polyad with $N = 1$ is referred to as either the first triad of 1δ and it contains three vibrational states, namely $(1, 0, 0)$, $(0, 2, 0)$ and $(0, 0, 1)$, where this notation is used to denote quanta of vibrational excitation, (n_1, n_2, n_3). The second polyad is like the first but has an extra quantum of excitation of the bending vibration, ν_2. This is known as the second triad or $1\delta + \nu$ and contains the three states $(1, 1, 0)$, $(0, 3, 0)$ and $(0, 1, 1)$. Water polyads are important not least because they are responsible for structure of absorbtion in the Earth's atmosphere with astronomical observing windows J, H, K, M. N and so forth lying in the gaps between these water bands.

Other molecules such as methane and ammonia also have a pronounced polyad structure. The structure of the methane polyads can clearly be seen in Fig. 3.16. This structure makes the rotation-vibration spectrum of methane appear fairly simple: this is not so. Each polyad is made up from a variety of different vibrational bands which, because they overlap, are hard or even impossible to disentangle. Understanding the observed spectrum of methane, particularly at near-infrared and red wavelengths, remains an active topic of research which is important for studies of exoplanets.

Species such H_2O, NH_3 and CH_4 all have vibrations involving hydrogen stretches (one or more H atoms vibrating against the central heavy atom). These stretches usually involve a significant change in the dipole moment and are therefore strong. They generally absorb or emit in the mid-infrared at wavenumbers 2000 to 3000

cm^{-1} (3–5 μm). Unfortunately, due to water absorbing very strongly in this region, these motions are hard to study from the ground.

All polyatomic molecules possess at least one "infrared active" vibrational mode. That is they all have at least one mode for which dipole allowed vibrational excitation can occur. This means that all polyatomic molecules can be detected by their infrared spectrum. For some molecules, such as CH_4, CO_2 and H_3^+ this probably represents the only practical way to observe the species astronomically. However, not all modes are infrared active. In the case of H_3^+ for example it is only the ν_2 bending mode which distorts the molecule to create an instantaneous dipole that has an allowed infrared spectra.

Rotation-vibration spectra of linear polyatomic molecules such as HCN or acetylene (HCCH) have a similar P-branch and R-brand structure to linear diatomics such as CO, see Fig. 3.11. For some bands there is also also a Q-branch corresponding to transitions where $J' = J''$; Q-branches manifest themselves by a strong peak near the band centre as all the Q-branch transitions lie at approximately the same wavenumber. Q-branch features can be used for detection of molecules at low resolution.

The rotation-vibration spectra of non-linear polyatomic molecules, particularly asymmetric tops, tend to have a much less pronounced structure. A classic example of this is the spectrum of water which is broad and unstructured; even transitions with $\Delta J = 0$ are spread out over a range of transition frequencies due to the substructure of the rotational levels.
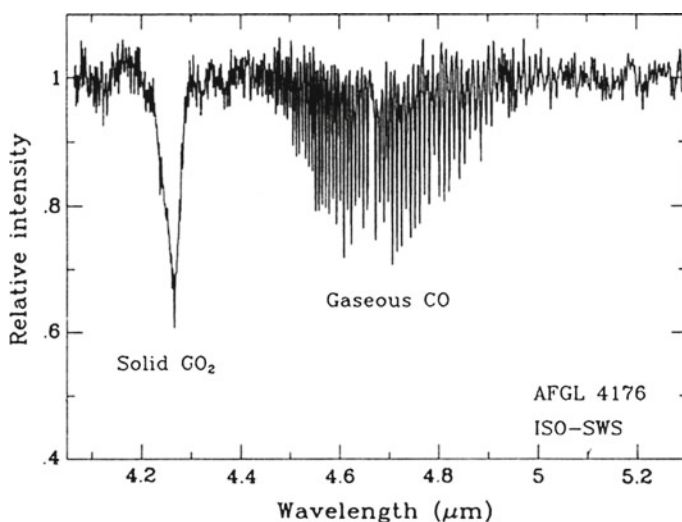

Fig. 3.13 Spectrum obtained with the Infrared Space Observatory toward the massive young stellar object AFGL 4176 in a dense molecular cloud. The strong, broad absorption at 4.27 μm is due to solid CO_2, whereas the structure at 4.4-4.9 μm indicates the presence of warm, gaseous CO along the line of sight. (Reproduced with permission from E.F. van Dishoeck, in *The Molecular Astrophysics of Stars and Galaxies*, eds. T.W. Hartquist and D.A. Williams (Clarendon Press, Oxford, 1998).)

Figure 3.13 shows an absorption spectrum of carbon monoxide recorded looking towards the massive young stellar object AFGL 4176, which is embedded in a dense molecular cloud. The shorter wavelength feature, which is due to solid carbon dioxide, shows how different these largely structureless condensed phase spectra are. The $4.7\,\mu$m region is heavily obscured by the Earth's atmosphere. This spectrum was recorded by a satellite, the Infrared Space Observatory (ISO).

3.5.3 Isotopologues

Isotopic substitution of molecules alters their rotation-vibration spectrum. As the vibrational frequency depends on the inverse square root of the molecular mass, see Eq. (3.16), these frequencies shift significantly upon isotopic substitution. These shifts can be resolved at reasonable resolution. Remember, however, that pure rotational spectra depend on the actual inverse of mass meaning that the shifts in the rotational transition frequencies are larger than those in rotation-vibration spectra.

There is one other important effect of isotopic substitution. Equation (3.15) shows that even in the $v = 0$ state there is a residual vibrational energy. This is known as the zero point energy and, like the transition frequencies, depends on the isotopic mass. This means isotopic substitution can change the energy of the system leading to an effect known as fractionation.

Consider the isotope exchange reaction:

$$D + H_2 \leftrightarrow H + HD. \tag{3.17}$$

The zero point energy of H_2, which is approximately 2200 cm^{-1}, exceeds that of HD, which is about 1905 cm^{-1}. This means that the reaction is exothermic by about 295 cm^{-1} or about 420 K. This means that at low temperatures the formation of HD is heavily favoured.

3.5.4 Molecular Hydrogen

H_2 has no permanent dipole moment so cannot undergo electric dipole-allowed vibration-rotation transitions.

However, there is a lot of hydrogen in the Universe. This means that very weak electric quadrupole transitions can occur instead. These are very weak: about a factor 10^{-8} weaker than dipole allowed transitions. The quadrupole transitions obey new selection rules: $\Delta J = +2$ which constitute the S-branch and $\Delta J = -2$ give the O-branch, as well as $\Delta J = 0$ transitions giving a Q-branch. H_2 transitions can be easily observed astronomically.

The infrared spectrum of Uranus is dominated by lines belonging to the fundamental ($v = 1 - 0$) rotation-vibration band of H_2. Figure 3.14 shows bright emission
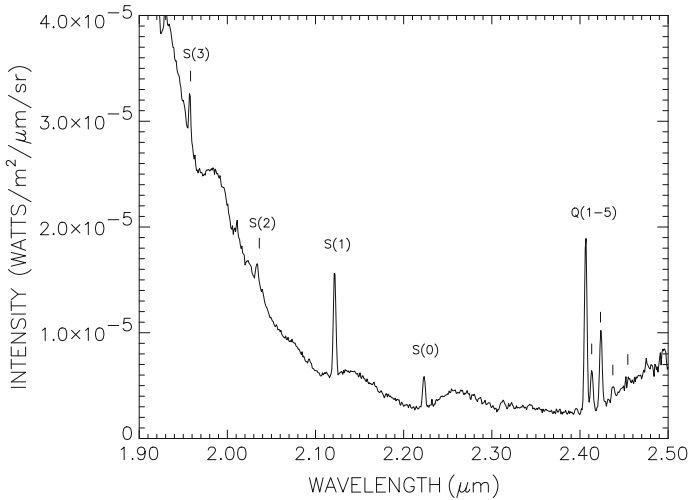
Fig. 3.14 K band infrared spectrum of Uranus showing H_2 quadrupole emission lines, adapted from Trafton et al. (1999)

lines, which are labeled, from both the S-branch ($\Delta J = +2$) and Q-branch ($\Delta J = 0$). The notation for assignments is S(J'') and Q(J''), where J'' is the rotational quantum number of the lower vibration state.

3.5.5 Temperature Effects

At room temperature most small molecules are predominantly in their vibrational ground state so spectra are dominated by transitions from this state. At higher temperatures, for example at temperatures found in the atmospheres of most exoplanets, higher vibrational states can become occupied. This leads to dramatic changes in the absorption spectrum.

Figure 3.15 compares the absorption spectrum of carbon monoxide at room temperature and at the temperature of a hot exoplanet. The figure shows the fundamental band about 2000 cm^{-1} plus the $v = 2 - 0$ and $v = 3 - 0$ overtone bands (note the standard notation is upper – lower). The cross section units are those adopted by the HITRAN data base of Gordon et al. (2017) and are macroscopic which means they require multiplication by Avogadro's number ($N_A = 6.022140857 \times 10^{23}$) to place them on a per molecule basis. The figure uses line-broadening parameters which results individual lines being blended into a single feature; however at 300 K the distinct P and R branches associated with each band can be seen. As the temperature is raised the peak of each band is reduced but the bands become significantly
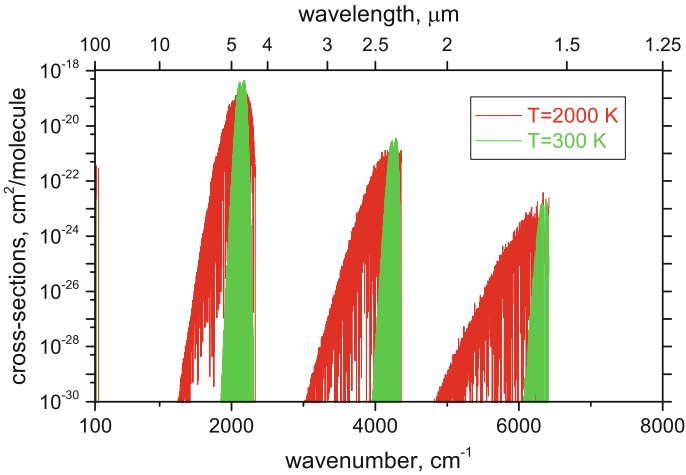
Fig. 3.15 Infrared absorption spectrum of carbon monoxide (CO) at 300 and 2000 K generated using the line list of Li et al. (2015)

broader. The integrated intensity of each band is roughly conserved as a function of temperature although it is difficult to judge this because of the log cross-section scale.

The broadening of the band with increasing temperature is caused by two effects. First more rotational levels are thermally occupied making the P and R branches broader. In practice the rotation-vibration spectrum of CO has a band head (see discussion of electronic spectra below) and this means that the broadening is largely to the red as temperature increases. At high resolution this particular feature of CO facilitates its use as thermometer in the atmospheres of cool stars and similar bodies, see Jones et al. (2005). Secondly at elevated temperatures excited vibrational states of CO become thermally occupied resulting in what are called hot band transitions of the type $v = 2 - 1$, $v = 3 - 1$ and $v = 4 - 1$. Anharmonic effects mean that the centres of these bands lie at slightly lower frequencies and again the band is largely red shifted. In summary as temperature is increased there is an increase in the number of observable transitions with the result that the band peaks are lowered and the band is broadened. In the case of CO the broadening shows a pronounced asymmetry with increased width towards the red.

Figure 3.16 gives a similar plot for methane. In this case there is a huge increase in the number of lines with temperature. Models of brown dwarfs demonstrated that it was necessary to include billions of spectral lines of methane alone to obtain reliable results, see Yurchenko et al. (2014). This is an important result which is of great significance for models of hot exoplanets.

Like that of CO, the effect of raising the temperature is to lower the peak absorption and to significantly broaden the bands. Unlike CO, at higher temperatures the windows between the bands disappear leading to the differences between the peaks
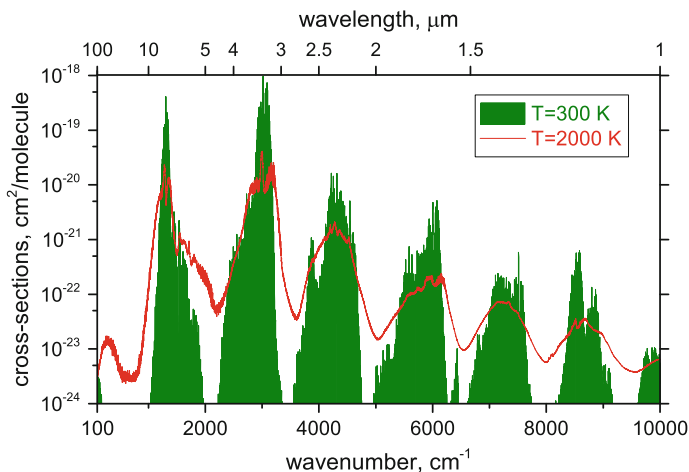
Fig. 3.16 Infrared absorption spectrum of methane (CH_4) at 300 and 2000 K generated using the 10 to 10 ExoMol line list of Yurchenko and Tennyson (2014)

and troughs being strongly flattened. This flattening is only achieved with very extensive line lists and is not given when, for example, a high temperature spectrum is modelled using a line list (such as those given by HITRAN) which are only complete for low temperatures. It was this realisation which led directly to the first successful detection of a molecule (water) in the atmosphere of a (hot Jupiter) exoplanet by Tinetti et al. (2007).

As for CO the lowering of the peaks and the flattening of the troughs in the hot methane spectrum is caused by a combination of high J rotational transitions and vibrational hot bands. In practice in polyatomic systems, starting from vibrationally excited states opens many new possibilities of transitions involving not only hot bands but also combination and difference bands. The net effect is to make both absorption and emission spectra of hot polyatomic molecules much flatter than the equivalent low temperature spectra. This has important consequences for both detection of these molecules, which is harder as the peaks are less pronounced, and radiative transport models as the opacity of hot molecules is widely distributed leading to blanket absorption. This can lead to trapping of radiation and significant increases in the size of atmospheres of bodies such as cool stars.

The large amount of data present in hot molecular line lists has led to treatments which lead to a more compact representation of the data. As the line list for a given molecule can be partitioned into strong and weak lines, the idea of representing the many, many weak lines using so-called super lines was suggested by Rey et al. (2017). An extensive discussion of this is given by Yurchenko et al. (2017).

3.6 Electronic Spectra

Electronic spectra involve a change of electronic state which corresponds to all spectra for atoms, which do not have the possibility of changes in vibrational or rotational motion. Important electronic spectra for standard closed-shell molecules such as all the molecules mentioned thus largely lie at ultra-violet wavelengths. However there is an important class of molecules which absorb at near-infrared or visible wavelengths. These are diatomic molecules containing a transition metal whose ground states are open shells. Open shells means that not all the electrons are paired and results in ground electronic states that are not $^1\Sigma^+$ states (see below for a discussion of this notation). Prominent examples of such species are TiO, VO, TiH and FeH. The spectrum of titanium monoxide (TiO) is particularly important as it is one of two major absorbers in the atmospheres of (cool) M-dwarf stars, the other important species is water (see Allard et al. 2000). These stars are the commonest ones in the local region of the Milky Way.

3.6.1 Electronc State Notation

For diatomic molecules the electronic state notation used for molecules has similarities to that used for atoms. The leading superscript is the electron spin degeneracy given as $2S + 1$ where S is the electron spin, as for atoms. This is followed by a letter designating the projection of the orbital angular momentum along the molecular axis, Λ. Here the Greek letters $\Sigma, \Pi, \Delta, \Phi, \ldots$ representing $\Lambda = 0, 1, 2, 3, \ldots$, respectively, correspond to the atomic S, P, D, F, …notation for states with $L = 0, 1, 2, 3, \ldots$. This means that a $^1\Sigma^+$ state has no spin or orbital angular momentum as it corresponds to $S = \Lambda = 0$. This situation is referred to by chemists as a closed shell and most stable diatomics are closed shell species. Conversely a $^2\Pi$ state has both electron spin, $S = \frac{1}{2}$, and orbital angular momentum, $\Lambda = 1$.

As there are many states (actually an infinite number) of a given orbital-spin symmetry, each state is also given an additional, leading state label. X is used for ground electronic states e.g. X $^1\Sigma^+$. States with the same spin degeneracy as the ground state are labelled A, B, C, …from the lowest upwards, and those of different spin degeneracy are designated a, b, c, …. Unfortunately this notation is only applied in a rather haphazard fashion with a large number of, normally historical, anomalies.

Of course, besides an electronic state designation, each molecule state belongs to a particular vibrational and rotational state and so needs v and J quantum numbers to be fully specified.

Table 3.5 Selection rules for spectra of diatomic molecules undergoing allowed electric dipole transitions

Rotations	$\Delta J = \pm 1$	for $\Lambda = 0-0$,
	$\Delta J = 0, \pm 1$	not $J = 0-0$, for other $\Delta \Lambda$
Vibrations	Δv any (Franck-Condon approximation)	
Spin	$\Delta S = 0$	
Orbital	$\Delta \Lambda = 0, \pm 1.$	
Σ states	$\Sigma^+ \leftrightarrow \Sigma^+$,	
	$\Sigma^- \leftrightarrow \Sigma^-$	
Symmetry	$g \leftrightarrow u$	Homonuclear molecules only

3.6.2 Selection Rules

Selection rules for rotation-vibration-electronic transitions are given in Table 3.5. These transitions are often characterised by the portmanteau word rovibronic. Note that as transitions within an electronic state are explicitly allowed, the table also covers the cases of pure-rotational transitions and rotation-vibration transitions which are discussed above. The main rules for changes in electronic states for diatomic molecules are $\Delta S = 0$, $\Delta \Lambda = 0, \pm 1$. In addition, homonuclear diatomic molecules such as H_2 have an extra symmetry label according to whether the electronic state is symmetric (gerade or "g") or anti-symmetric (ungerade or "u"). This selection rule, which mirrors the Laporte rule for parity changes in atomic transitions, states that only g $\leftrightarrow$ u transitions are allowed.

There is no formal selection rule on vibrational transitions between different electronic states. Instead there are propensities which are controlled by the squared overlap of the vibrational wavefunctions in the upper and lower states. These terms, which are known as Franck-Condon factors, suggest that if two electronic states are approximately parallel then $\Delta v = 0$ transitions are strongly favoured. This is not the most common case and the reader is referred to Bernath (2015) for a more detailed discussion.

3.6.3 Band Structure

Rovibronic transitions like rotation-vibration ones obey the simple rotational selection that $\Delta J = 0, \pm 1$. However even for diatomic molecules, this may not lead to simple structures in the spectrum. This because the bondlength in the two electronic states involved in the transitions usually differ, resulting in very different rotational constants, see Eq. (3.10). This means that instead of the rotational structure producing a clear regular structure, the band tends to close-up in either the P or R branch resulting in the formation of a sharp feature known as a band head. Figure 3.17 shows
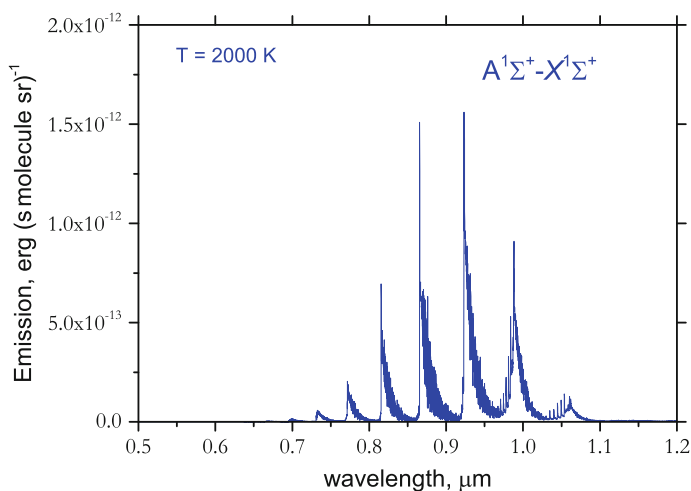
Fig. 3.17 Emission spectrum from the CaO A $^1\Sigma^+$ – X $^1\Sigma^+$ band of CaO at a temperature of 2000 K generated using the VBATHY ExoMol line list of Yurchenko et al. (2016a)

an emission spectrum for CaO; the spectrum shows clear band heads. These band heads can provide molecular markers even at relatively low resolution.

3.6.4   *Duo*

For exoplanet studies it has so far been found that electronic spectra of importance belong to diatomic species. Computing the spectra of diatomics from given potential energy curves is in principle straightforward. For closed shell species the program Level due to Le Roy (2017) has long provided an excellent means of computing spectra.

However, the spectra of open shell molecules are significantly more complex due to need to consider the various angular momentum couplings that arise between the rotational, spin and electronic angular momentum, see Tennyson et al. (2016b) for a comprehensive discussion of these. Yurchenko et al. (2016b) developed a new general diatomic code called Duo for computing rovibronic spectra of diatomic molecules and based on a rigorous treatment of these couplings in diatomic systems. Duo is freely available from the CCPforge program depository (ccpforge.cse.rl.ac.uk).

3.6.5   *Molecular Hydrogen*

H$_2$ has a number of strong electronic bands. The most prominent are the Werner (C $^1\Pi_u$ – X $^1\Sigma_g^+$) and the Lyman (B $^1\Sigma_u^+$ – X $^1\Sigma_g^+$) bands. Note that the H$_2$ Lyman band

is distinct from H atom Lyman lines. These bands are strong but lie in ultraviolet regions which means that they can only be observed from space.

3.7 Line Profiles

Spectral lines do not occur as a completely sharp feature at a unique frequency, instead each line has a profile. This profile is made up of a number of contributions:

1. Natural broadening: because each excited state has a finite lifetime, the uncertainty principle dictates that it must also have a finite spread (uncertainty) in its energy. This leads to a Lorentzian line profile. However, natural broadening is generally very small and is therefore only significant for the most precise laboratory measurements, Natural broadening is normally ignored for astronomical observations.
2. Doppler broadening: due to thermal motion of the molecules. This is distinct from Doppler shifts such as the red-shift which are due to overall motion of the body of gas being observed. Doppler broadening gives a Gaussian line profile which depends only on the (translational) temperature of the species concerned and its mass.
3. Pressure broadening: molecules in an atmosphere experience constant collisions due to the bombardment by other species present in the atmosphere. These collisions leads to small changes to the environment in which a transition occurs and hence to both pressure broadening of the transition and small shifts in the line position. The effect on the line shape can approximately be represented by a Lorentzian profile. The width of this profile of course depends on the pressure but also nature of the colliding species and the quantum numbers of the states involved in the transition. In practice, it is found for molecules that pressure-broadening depends more strongly on rotational state than on the precise vibrational states involved. In particular pressure effects decrease with rotational excitation. Pressure can also lead to mixing between lines. Line-mixing effects are particularly important when transitions lie close together, such as in Q-branches. However, this process can probably be ignored in most astronomical applications.
4. Other effects: lines are also broadened and shifted in the presence of electron collisions, this is particularly true for ions for which the interactions are long-range. As discussed above, magnetic fields can lead to a splitting in spectral lines: if the field is weak or the splitting is not resolved, this can also appear as a line broadening effect.

The most important effects in planetary atmospheres are due to Doppler and pressure broadening. As these effects depend respectively on Gaussian and Lorentzian profiles, the two effects need to be convolved. The standard convolution is the so-called Voigt profile and this is the one routinely used in models of planetary atmospheres. The Voigt profile is not analytic but there are a number of procedures available for evaluating it.

The pressure part of the Voigt profile also requires data for each transition and broadening. There is a severe lack of reliable information on broadening by key species such as H_2 and He, particularly at the elevated temperatures found, for example, in hot Jupiter exoplanets.

The effect of using a Voigt profile is to re-distribute the net absorption but, if the line is optically thin, the overall flux absorbed does not change. This is not true for optically thick lines for which the degree of broadening is crucial in determining the net absorption. Given that observations of exoplanets in primary transit give rise to long atmospheric pathlengths across the limb of the planet, it is inevitable that at least some of the lines will become optically thick. The importance of broadening under these circumstances has been demonstrated by Tinetti et al. (2012), who showed that pressure effects were particularly strong for long wavelength transitions.

In practice the Voigt profile is only an approximation to the true line profile as there are a number of subtle collisional effects which need to be considered to fully reproduce observed line-shapes, see Tennyson et al. (2014). Both Hartmann et al. (2008) and Buldyreva et al. (2010) provide comprehensive textbooks on line broadening to which the reader is referred for more information.

3.8 Spectroscopic Database

Access to data is an important issue for astronomical models. This section considers some useful sources of data. In principle the virtual atomic and molecular data centre (VAMDC) portal of Dubernet et al. (2016) provides access to the key spectroscopic data (and useful collision data) for astrophysical problems. However many of the datasets needed for molecular spectroscopy are too large to be handled by VAMDC; in this case it is necessary to go to the actual database.

3.8.1 Ground Rules

Before considering data sources in detail, it is worth considering some basic rules of what data to use and how to use them.

The HITRAN database, discussed further below, has been honed for many years to meet the needs of the large scientific community interested in studies of the Earth's atmosphere. It is an excellent source of data but explicitly designed to work at Earth temperatures. Indeed the data representation is all based on a reference temperature of 296 K. The nature of spectroscopic data is such that HITRAN data are probably suitable for modelling Earth-like objects at lower temperatures. However, at higher temperatures molecular spectra involve many more lines than are in HITRAN and use of the line lists provided by HITRAN will lead to spectroscopic features which are both systematically missing flux and, perhaps even more importantly, have the wrong band profiles.

Modellers should follow the following simple rules:

1. When modelling an Earth-like planet at temperatures below about 400 K HITRAN provides and excellent source of data.
2. When modelling temperatures above 400 K do not use HITRAN data.
3. When modelling data for hydrogen-rich systems such as gas giants data have to be taken from sources other than HITRAN, which does not aim to complete even for cool systems which are not oxygen-rich, such as Titan.
4. Do not claim that data come from HITRAN when they do not! This point may seem obvious but unfortunately there are frequent occurrence in the literature of this happening.
5. Equally obvious, but also ignored: cite the data sources used.

3.8.2 Atomic Data Sources

The NIST Atomic Spectra Database (https://www.nist.gov/pml/atomic-spectra-database) provides an excellent source of atomic spectroscopic data. It contains detailed listings of atomic energy levels (term values) and Einstein A coefficients (transition probabilities). In addition the Vienna atomic line database (VALD), see Ryabchikova et al. (2015), TOPbase (Cunto et al. 1993) and the extensive compilations due to Kurucz (2011) provide comprehensive data on ions important for stellar models.

3.8.3 The ExoMol Project

The ExoMol project was started by Tennyson and Yurchenko (2012) with the explicit aim of providing comprehensive molecular line lists for exoplanet and other atmospheres, Table 3.6 lists the currently available ExoMol molecular line lists. Table 3.7 list other line lists also available from the ExoMol website (www.exomol.com).

The ExoMol database, as described by Tennyson et al. (2016c), contains a number of features useful for models and other activities:

1. The database has a fully-configured applications program interface (API) which allows data, which can be dynamically updated, to be read directly into an application program.
2. Cross sections as function of temperature are presented for zero pressure and in many cases for H_2/He atmospheres.
3. Partition functions valid up to high temperatures are presented.
4. Pressure broadening parameters for H_2 and He as a function of temperature and rotational quantum are presented using the so-called ExoMol diet of Barton et al. (2017).
5. Tables of k-coefficients are presented for key species.

Table 3.6 Datasets created by the ExoMol project and included in the ExoMol database

Paper	Molecule	N_{iso}	T_{max}	N_{elec}	N_{lines}	DSName	Reference
I	BeH	1	2000	1	16 400	Yadin	Yadin et al. (2012)
I	MgH	3	2000	1	10 354	Yadin	Yadin et al. (2012)
I	CaH	1	2000	1	15 278	Yadin	Yadin et al. (2012)
II	SiO	5	9000	1	254 675	EJBT	Barton et al. (2013)
III	HCN/HNC	2[a]	4000	1	399 000 000	Harris	Barber et al. (2014)
IV	CH_4	1	1500	1	9 819 605 160	YT10to10	Yurchenko and Tennyson (2014)
V	NaCl	2	3000	1	702 271	Barton	Barton et al. (2014)
V	KCl	4	3000	1	1 326 765	Barton	Barton et al. (2014)
VI	PN	2	5000	1	142 512	YYLT	Yorke et al. (2014)
VI	PH_3	1	1500	1	16 803 703 395	SAlTY	Sousa-Silva et al. (2015)
VIII	H_2CO	1	1500	1	10 000 000 000	AYTY	Al-Refaie et al. (2015)
IX	AlO	4	8000	3	4 945 580	ATP	Patrascu et al. (2015)
X	NaH	2	7000	2	79 898	Rivlin	Rivlin et al. (2015)
XI	HNO_3	1	500	1	6 722 136 109	AIJS	Pavlyuchko et al. (2015)
XII	CS	8	3000	1	548 312	JnK	Paulose et al. (2015)
XIII	CaO	1	5000	5	21 279 299	VBATHY	Yurchenko et al. (2016a)
XIV	SO_2	1	2000	1	1 300 000 000	ExoAmes	Underwood et al. (2016b)
XV	H_2O_2	1	1250	1	20 000 000 000	APTY	Al-Refaie et al. (2016)
XIV	H_2S	1	2000	1	115 530 3730	AYTY	Azzam et al. (2016)
XV	SO_3	1	800	1	21 000 000 000	UYT2	Underwood et al. (2016a)
XVI	VO	1	2000	13	277 131 624	VOMYT	McKemmish et al. (2016)
XIX	$H_2^{17,18}O$	4[b]	3000	1	1 500 000 000	HotWat78	Polyansky et al. (2017)
XX	H_3^+	2[c]	3000	1	11 500 000 000	MiZATeP	Mizus et al. (2017)
XXI	NO	6	5000	2	2 281 042	NOName	Wong et al. (2017)
XXII	SiH_4	1	1200	1	62 690 449 078	OY2T	Owens et al. (2017a)
XXIII	PO	1	3000	1	1 500 000 000	POPS	Prajapat et al. (2017)
XXIII	PS	1	3000	3	1 500 000 000	POPS	Prajapat et al. (2017)
XXIV	SiH	4	5000	3	1 724 841	SiGHTLY	Yurchenko et al. (2018a)

N_{iso} Number of isotopologues considered;
T_{max} Maximum temperature for which the line list is complete;
N_{elec} Number of electronic states considered;
N_{lines} Number of lines: value is for the main isotope.
DSName Data set name for that line list.
[a] A line list for $H^{13}CN/HN^{13}C$ due to Harris et al. (2008) is also available.
[b] Line lists for $H_2^{16}O$ (BT2) due to Barber et al. (2006) $HD^{16}O$ (VTT) due to Voronin et al. (2010) are also available.
[c] A line list for H_2D^+ due to Sochi and Tennyson (2010) is also available

6. State-resolved lifetimes are presented for each species, see Tennyson et al. (2016a). These lifetimes can be used to obtain critical densities amongst other things.
7. Temperature-dependent cooling functions are presented.

Table 3.7 Other molecular line lists which can be obtained from the ExoMol website

Molecule	N_{iso}	T_{max}	N_{elec}	N_{lines}	DSName	Reference	Methodology
H_2O	2^a	3000	1	505 806 202	BT2	Barber et al. (2006)	ExoMol
NH_3	2^b	1500	1	1 138 323 351	BYTe	Yurchenko et al. (2011)	ExoMol
HeH^+	4	10000	1	1 431	Engel	Engel et al. (2005)	Ab initio
HD^+	1	12000	1	10 119	CLT	Coppola et al. (2011)	Ab initio
LiH	1	12000	1	18 982	CLT	Coppola et al. (2011)	Ab initio
LiH^+	1	12000	1	332	CLT	Coppola et al. (2011)	Ab initio
ScH	1	5000	6	1 152 827	LYT	Lodi et al. (2015)	Ab initio
MgH	1		3	30 896	13GhShBe	GharibNezhad et al. (2013)	Empirical
CaH	1		2	6000	11LiHaRa	Li et al. (2012)	Empirical
NH	1		1	10 414	14BrBeWe	Brooke et al. (2014a)	Empirical
CH	2		4	54 086	14MaPlVa	Masseron et al. (2014)	Empirical
CO	9	9000	1	752 976	15LiGoRo	Li et al. (2015)	Empirical
OH	1	6000	1	45 000	16BrBeWe	Brooke et al. (2016)	Empirical
CN	1		1	195 120	14BrRaWe	Brooke et al. (2014b)	Empirical
CP	1		1	28 735	14RaBrWe	Ram et al. (2014)	Empirical
HCl	1		1	2588	11LiGoBe	Li et al. (2011)	Empirical
CrH	1		2	13 824	02BuRaBe	Burrows et al. (2002)	Empirical
FeH	1		2	93 040	10WeReSe	Wende et al. (2010)	Empirical
TiH	1		3	181 080	05BuDuBa	Burrows et al. (2005)	Empirical

N_{iso} Number of isotopologues considered;
T_{max} Maximum temperature for which the line list is complete;
N_{elec} Number of electronic states considered;
N_{lines} Number of lines: value is for the main isotope.
[a] The VTT line list for HDO due to Voronin et al. (2010) is also available.
[b] There is a room temperature $^{15}NH_3$ line list due to Yurchenko (2015)

8. Landé *g*-factors are given for open shell diatomic molecules, see Semenov et al.
   (2017),
9. Finally, transition dipoles are stored; these are being used for studies of molecular
   control/orientation effects, aee Owens et al. (2017b). In future this information
   could also be useful for studies of polarisation effects.

In addition the program ExoCross of Yurchenko et al. (2018b) can be used to process
line lists and to convert between ExoMol and HITRAN formats. Data can also con-
verted to the Phoenix format of Jack et al. (2009), which is widely used for brown
dwarf and other models.

3.8.4 Other Data Sources

As discussed above the HITRAN database contains comprehensive sets of spec-
troscopic parameters. The 2016 HITRAN release of Gordon et al. (2017) contains
line-by-line data for 49 molecules of importance to models of the Earth's atmosphere

plus a very extensive set of cross sections for larger molecules. In particular these cross sections have subsumed the PNNL library of Sharpe et al. (2004). HITRAN data are designed for use at terrestrial temperatures; the HITEMP database of Rothman et al. (2010) is designed to extend HITRAN to higher temperatures. However, HITEMP only contains data for five molecules: water, CO_2, CO, OH and NO. Newer and improved line lists are available for these species making HITEMP essentially redundant; release of a new edition of HITEMP is overdue.

The GEISA database of Jacquinet-Husson et al. (2016) contains data on 52 species. GEISA is very similar in design and content to HITRAN although it does contain some line data on carbon-containing molecules not included in HITRAN.

The compilations by Kurucz (2011) contains some data on diatomic molecules largely based on use of the diatomic constants given by Huber and Herzberg (1979). These data are not particularly accurate but are useful when no other data are available. Similarly the recent release of VALD (Ryabchikova et al. 2015) contains line list for a few diatomics as generated by Plez.

Other data sources includes the TheoReTS database of Rey et al. (2016) which is particularly useful for hot hydrocarbon species. The group at NASA Ames have generated extensive datasets for hot molecules found in the atmospheres of Venus and Mars, including recent line lists for all major isotopologues of CO_2 (Huang et al. 2017). Bernath and co-workers have assembled extensive empirical line lists for a variety of molecules, most of these are available via the ExoMol website, see Table 3.7.

3.9 Conclusion

To understand the spectroscopic signatures of atoms and molecules in the atmospheres of planets and elsewhere requires a wealth of spectroscopic data. This chapter gives a brief introduction to the physics involved in the various spectroscopic processes encountered in atoms and molecules. Of necessity many important issues are dealt with only briefly or not at all. However, I have tried to point to both sources of further information on the topic and useful sources of spectroscopic data for studies of exoplanets. I would like to end with one more comment. Any model is only as good as the data input into it. The use of good laboratory data is therefore crucial. Equally important when presenting results is to provide the source of these data. Not to do so is both to make any results presented unreproducible and to cast doubt on the validity of any results because of the unknown provenance of the data employed. In short: please cite your data sources.

References

Al-Refaie, A.F., Yurchenko, S.N., Yachmenev, A., Tennyson, J.: MNRAS **448**, 1704 (2015)

Al-Refaie, A.F., Polyansky, O.L., Ovsyannikov, R.I., Tennyson, J., Yurchenko, S.N.: MNRAS **461**, 1012 (2016)

Allard, F., Hauschildt, P.H., Schwenke, D.: ApJ **540**, 1005 (2000)

Azzam, A.A.A., Yurchenko, S.N., Tennyson, J., Naumenko, O.V.: MNRAS **460**, 4063 (2016)

Barber, R.J., Tennyson, J., Harris, G.J., Tolchenov, R.N.: MNRAS **368**, 1087 (2006)

Barber, R.J., Strange, J.K., Hill, C., Polyansky, O.L., Mellau, G.C., Yurchenko, S.N., Tennyson, J.: MNRAS **437**, 1828 (2014)

Barklem, P.S., Collet, R.: A&A **588**, A96 (2016)

Barton, E.J., Yurchenko, S.N., Tennyson, J.: MNRAS **434**, 1469 (2013)

Barton, E.J., Chiu, C., Golpayegani, S., Yurchenko, S.N., Tennyson, J., Frohman, D.J., Bernath, P.F.: MNRAS **442**, 1821 (2014)

Barton, E.J., Hill, C., Czurylo, M., Li, H.Y., Hyslop, A., Yurchenko, S.N., Tennyson, J.: J. Quant. Spectrosc. Radiat. Transf. **203**, 490 (2017)

Berdyugina, S.V., Solanki, S.K.: A&A **365**, 701 (2002)

Berdyugina, S.V., Braun, P.A., Fluri, D.M., Solanki, S.K.: A&A **444**, 947 (2005)

Bernath, P.F.: Spectra of Atoms and Molecules, 3rd edn. Oxford University Press (2015)

Bray, C., Cuisset, A., Hindle, F., Mouret, G., Bocquet, R., Boudon, V.: J. Quant. Spectrosc. Radiat. Transf. **203**, 349 (2017)

Brooke, J.S.A., Bernath, P.F., Western, C.M., van Hemert, M.C., Groenenboom, G.C.: J. Chem. Phys. **141**, 054310 (2014a)

Brooke, J.S.A., Ram, R.S., Western, C.M., Li, G., Schwenke, D.W., Bernath, P.F.: ApJS **210**, 23 (2014b)

Brooke, J.S.A., Bernath, P.F., Western, C.M., Sneden, C., Afsar, M., Li, G., Gordon, I.E.: J. Quant. Spectrosc. Radiat. Transf. **138**, 142 (2016)

Brown, J.M., Carrington A.: Rotational Spectroscopy of Diatomic Molecules. Cambridge University Press (2003)

Buldyreva, J., Lavrentieva, N., Starikov, V.: Collisional Line Broadening and Shifting of Atmospheric Gases: A Practical Guide for Line Shape Modelling by Current Semi-classical Approaches. Imperial College Press, London (2010)

Burrows, A., Ram, R.S., Bernath, P., Sharp, C.M., Milsom, J.A.: ApJ **577**, 986 (2002)

Burrows, A., Dulick, M., Bauschlicher, C.W., Bernath, P.F., Ram, R.S., Sharp, C.M., Milsom, J.A.: ApJ **624**, 988 (2005)

Cauley, P.W., Redfield, S., Jensen, A.G.: ApJ **153**, 81 (2017)

Coppola, C.M., Lodi, L., Tennyson, J.: MNRAS **415**, 487 (2011)

Cunto, W., Mendoza, C., Ochsenbein, E., Zeippen, C.J.: A&A **275**, L5 (1993)

Dello Russo, N., Bonev, B.P., DiSanti, M.A., Gibb, E.L., Mumma, M.J., Magee-Sauer, K., Barber, R.J., Tennyson, J.: ApJ **621**, 537 (2005)

Drossart, P., Maillard, J.P., Caldwell, J., et al.: Nature **340**, 539 (1989)

Dubernet, M.L., Antony, B.K., Ba, Y.A., et al.: J. Phys. B: At. Mol. Opt. Phys. **49**, 074003 (2016)

Engel, E.A., Doss, N., Harris, G.J., Tennyson, J.: MNRAS **357**, 471 (2005)

Gamache, R.R., Roller, C., Lopes, E., et al.: J. Quant. Spectrosc. Radiat. Transf. **203**, 70 (2017)

GharibNezhad, E., Shayesteh, A., Bernath, P.F.: MNRAS **432**, 2043 (2013)

Gordon, I.E., Rothman, L.S., Babikov, Y., et al.: J. Quant. Spectrosc. Radiat. Transf. **203**, 3 (2017)

Harris, G.J., Larner, F.C., Tennyson, J., Kaminsky, B.M., Pavlenko, Y.V., Jones, H.R.A.: MNRAS **390**, 143 (2008)

Hartmann, J.M., Boulet, C., Robert, D.: Collisional effects on molecular spectra. Laboratory experiments and models, consequences for applications. Elsevier, Amsterdam (2008)

Huang, X., Schwenke, D.W., Freedman, R.S., Lee, T.J.: J. Quant. Spectrosc. Radiat. Transf. **203**, 224 (2017)

Huber, K.P., Herzberg, G.: Molecular Spectra and Molecular Structure IV. Constants of Diatomic Molecules. Van Nostrand Reinhold Company, New York (1979)

Irwin, A.W.: ApJS **45**, 633 (1981)

Jack, D., Hauschildt, P.H., Baron, E.: A&A **502**, 1043 (2009)

Jacquinet-Husson, N., Armante, R., Scott, N.A., et al.: J. Mol. Spectrosc. **327**, 31 (2016)

Jones, H.R.A., Pavlenko, Y., Viti, S., Barber, R.J., Yakovina, L., Pinfold, D., Tennyson, J.: MNRAS **358**, 105 (2005)

Kurucz, R.L.: Can. J. Phys. **89**, 417 (2011)

Le Roy, R.J.: J. Quant. Spectrosc. Radiat. Transf. **186**, 167 (2017)

Lellouch, E., Gurwell, M., Butler, B., et al.: Icarus **286**, 289 (2017)

Li, G., Gordon, I.E., Bernath, P.F., Rothman, L.S.: J. Quant. Spectrosc. Radiat. Transf. **112**, 1543 (2011)

Li, G., Harrison, J.J., Ram, R.S., Western, C.M., Bernath, P.F.: J. Quant. Spectrosc. Radiat. Transf. **113**, 67 (2012)

Li, G., Gordon, I.E., Rothman, L.S., Tan, Y., Hu, S.M., Kassi, S., Campargue, A., Medvedev, E.S.: ApJS **216**, 15 (2015)

Lodi, L., Yurchenko, S.N., Tennyson, J.: Mol. Phys. **113**, 1559 (2015)

Masseron, T., Plez, B., Van Eck, S.: A&A **571**, A47 (2014)

McKemmish, L.K., Yurchenko, S.N., Tennyson, J.: MNRAS **463**, 771 (2016)

Miller, S., Tennyson, J.: ApJ **335**, 486 (1988)

Mizus, I.I., Alijah, A., Zobov, N.F., Kyuberis, A.A., Yurchenko, S.N., Tennyson, J., Polyansky, O.L.: MNRAS **468**, 1717 (2017)

Müller, H.S.P., Schlöder, F., Stutzki, J., Winnewisser, G.: J. Mol. Struct. (THEOCHEM) **742**, 215 (2005)

Owens, A., Yurchenko, S.N., Yachmenev, A., Thiel, W., Tennyson, J.: MNRAS **471**, 5025 (2017a)

Owens, A., Zak, E.J., Chubb, K.L., Yurchenko, S.N., Tennyson, J., Yachmenev, A.: Sci. Rep. **7**, 45068 (2017b)

Pachucki, K., Komasa, J.: Phys. Rev. A **78**, 052503 (2008)

Patrascu, A.T., Tennyson, J., Yurchenko, S.N.: MNRAS **449**, 3613 (2015)

Paulose, G., Barton, E.J., Yurchenko, S.N., Tennyson, J.: MNRAS **454**, 1931 (2015)

Pavlyuchko, A.I., Yurchenko, S.N., Tennyson, J.: MNRAS **452**, 1702 (2015)

Pickett, H.M., Poynter, R.L., Cohen, E.A., Delitsky, M.L., Pearson, J.C., Müller, H.S.P.: Quant. Spectrosc. Radiat. Transf. **60**, 883 (1998)

Polyansky, O.L., Zobov, N.F., Viti, S., Tennyson, J., Bernath, P.F., Wallace, L.: J. Mol. Spectrosc. **186**, 422 (1997)

Polyansky, O.L., Kyuberis, A.A., Lodi, L., Tennyson, J., Ovsyannikov, R.I., Zobov, N.: MNRAS **466**, 1363 (2017)

Pont, F., Sing, D.K., Gibson, N.P., Aigrain, S., Henry, G., Husnoo, N.: MNRAS **432**, 2917 (2013)

Prajapat, L., Jagoda, P., Lodi, L., Gorman, M.N., Yurchenko, S.N., Tennyson, J.: MNRAS **472**, 3648 (2017)

Ram, R.S., Brooke, J.S.A., Western, C.M., Bernath, P.F.: J. Quant. Spectrosc. Radiat. Transf. **138**, 107 (2014)

Rey, M., Nikitin, A.V., Babikov, Y.L., Tyuterev, V.G.: J. Mol. Struct. (Theochem) **327**, 138 (2016)

Rey, M., Nikitin, A.V., Tyuterev, V.G.: ApJ **847**, 105 (2017)

Rivlin, T., Lodi, L., Yurchenko, S.N., Tennyson, J., Le Roy, R.J.: MNRAS **451**, 5153 (2015)

Rothman, L.S., Gordon, I.E., Barber, R.J., et al.: J. Quant. Spectrosc. Radiat. Transf. **111**, 2139 (2010)

Ryabchikova, T., Piskunov, N., Kurucz, R.L., Stempels, H.C., Heiter, U., Pakhomov, Y., Barklem, P.S.: Phys. Scr. **90**, 054005 (2015)

Sauval, A.J., Tatum, J.B.: ApJS **56**, 193 (1984)

Semenov, M., Yurchenko, S.N., Tennyson, J.: J. Mol. Spectrosc. **330**, 57 (2017)

Sharpe, S.W., Johnson, T.J., Sams, R.L., Chu, P.M., Rhoderick, G.C., Johnson, P.A.: Appl. Spectrosc. **58**, 1452 (2004)

Sochi, T., Tennyson, J.: MNRAS **405**, 2345 (2010)

Sousa-Silva, C., Yurchenko, S.N., Tennyson, J.: J. Mol. Spectrosc. **288**, 28 (2013)

Sousa-Silva, C., Al-Refaie, A.F., Tennyson, J., Yurchenko, S.N.: MNRAS **446**, 2337 (2015)

Tennyson, J.: Astronomical Spectroscopy: An Introduction to the Atomic and Molecular Physics of Astronomical Spectra, 2nd edn. World Scientific, Singapore (2011)

Tennyson, J., Yurchenko, S.N.: MNRAS **425**, 21 (2012)

Tennyson, J., Bernath, P.F., Campargue, A., et al.: Pure. Appl. Chem. **86**, 1931 (2014)

Tennyson, J., Hulme, K., Naim, O.K., Yurchenko, S.N.: J. Phys. B: At. Mol. Opt. Phys. **49**, 044002 (2016a)

Tennyson, J., Lodi, L., McKemmish, L.K., Yurchenko, S.N.: J. Phys. B: At. Mol. Opt. Phys. **49**, 102001 (2016b)

Tennyson, J., Yurchenko, S.N., Al-Refaie, A.F., et al.: J. Mol. Spectrosc. **327**, 73 (2016c)

Tinetti, G., Vidal-Madjar, A., Liang, M.C., et al.: Nature **448**, 169 (2007)

Tinetti, G., Tennyson, J., Griffiths, C.A., Waldmann, I.: Phil. Trans. R. Soc. Lond. A **370**, 2749 (2012)

Townes, C.H., Schawlow, A.L.: Microwave Spectroscopy. Dover (2012)

Trafton, L.M., Miller, S., Geballe, T.R., Tennyson, J., Ballester, G.E.: ApJ **524**, 1059 (1999)

Underwood, D.S., Tennyson, J., Yurchenko, S.N., Clausen, S., Fateev, A.: MNRAS **462**, 4300 (2016a)

Underwood, D.S., Tennyson, J., Yurchenko, S.N., Huang, X., Schwenke, D.W., Lee, T.J., Clausen, S., Fateev, A.: MNRAS **459**, 3890 (2016b)

Vidal-Madjar, A., des Etangs, A.L., Desert, J.M., Ballester, G.E., Ferlet, R., Hebrand, G., Mayor, M.: Nature **422**, 143 (2003)

Vidler, M., Tennyson, J.: J. Chem. Phys. **113**, 9766 (2000)

Voronin, B.A., Tennyson, J., Tolchenov, R.N., Lugovskoy, A.A., Yurchenko, S.N.: MNRAS **402**, 492 (2010)

Wallace, L., Livingston, W., Hinkle, K., Bernath, P.: ApJS **106**, 165 (1996)

Wende, S., Reiners, A., Seifahrt, A., Bernath, P.F.: A&A **523**, A58 (2010)

Wenger, C., Champion, J.P.: J. Quant. Spectrosc. Radiat. Transf. **59**, 471 (1998)

Wong, A., Yurchenko, S.N., Bernath, P., Mueller, H.S.P., McConkey, S., Tennyson, J.: MNRAS **470**, 882 (2017)

Woodgate, G.K.: Elementary Atomic Structure, 2nd edn. Oxford University Press (1983)

Yadin, B., Vaness, T., Conti, P., Hill, C., Yurchenko, S.N., Tennyson, J.: MNRAS **425**, 34 (2012)

Yorke, L., Yurchenko, S.N., Lodi, L., Tennyson, J.: MNRAS **445**, 1383 (2014)

Yurchenko, S.N.: J. Quant. Spectrosc. Radiat. Transf. **152**, 28 (2015)

Yurchenko, S.N., Tennyson, J.: MNRAS **440**, 1649 (2014)

Yurchenko, S.N., Barber, R.J., Tennyson, J.: MNRAS **413**, 1828 (2011)

Yurchenko, S.N., Tennyson, J., Bailey, J., Hollis, M.D.J., Tinetti, G.: Proc. Nat. Acad. Sci. **111**, 9379 (2014)

Yurchenko, S.N., Blissett, A., Asari, U., Vasilios, M., Hill, C., Tennyson, J.: MNRAS **456**, 4524 (2016a)

Yurchenko, S.N., Lodi, L., Tennyson, J., Stolyarov, A.V.: Comput. Phys. Commun. **202**, 262 (2016b)

Yurchenko, S.N., Amundsen, D.S., Tennyson, J., Waldmann, I.P.: A&A **605**, A95 (2017)

Yurchenko, S.N., Sinden, F., Lodi, L., Hill, C., Gorman M.N., Tennyson, J.: MNRAS **473**, 5324 (2018a)

Yurchenko, S.N., Al-Refaie, A.F., Tennyson, J.: A&A (2018b)